Fotonica 2D
Difetti

Tipologia dei difetti

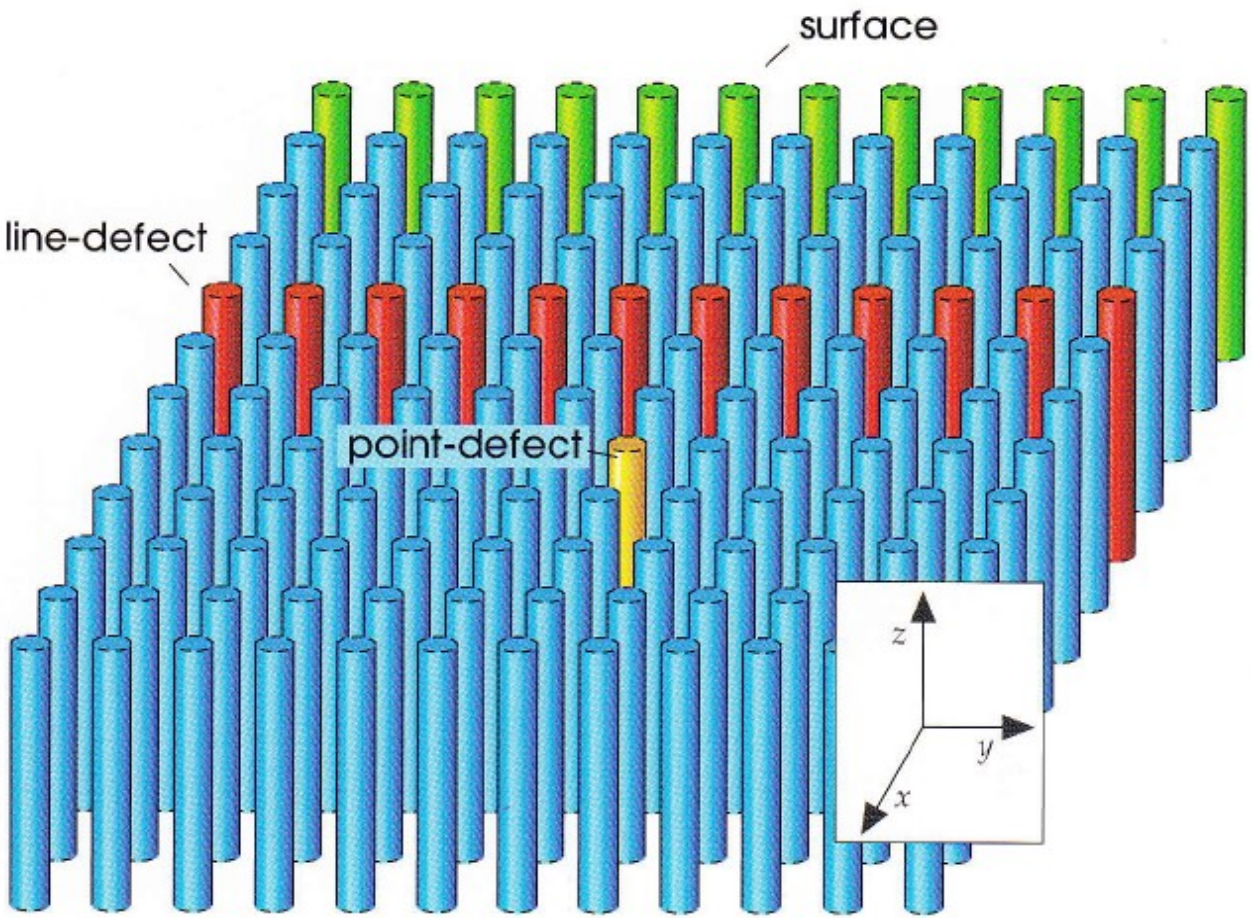

Figure 12: Schematic illustration of possible sites of point, line, and surface defects. Perturbing one column in the bulk of the crystal (yellow) might allow a defect state to be localized in both x and y. Perturbing one row in the bulk of the crystal (red) or truncating the crystal at a surface (green) might allow a state to be localized in one direction (x). The rods are assumed to extend indefinitely in the z direction.

Stati nel PGB (ED)

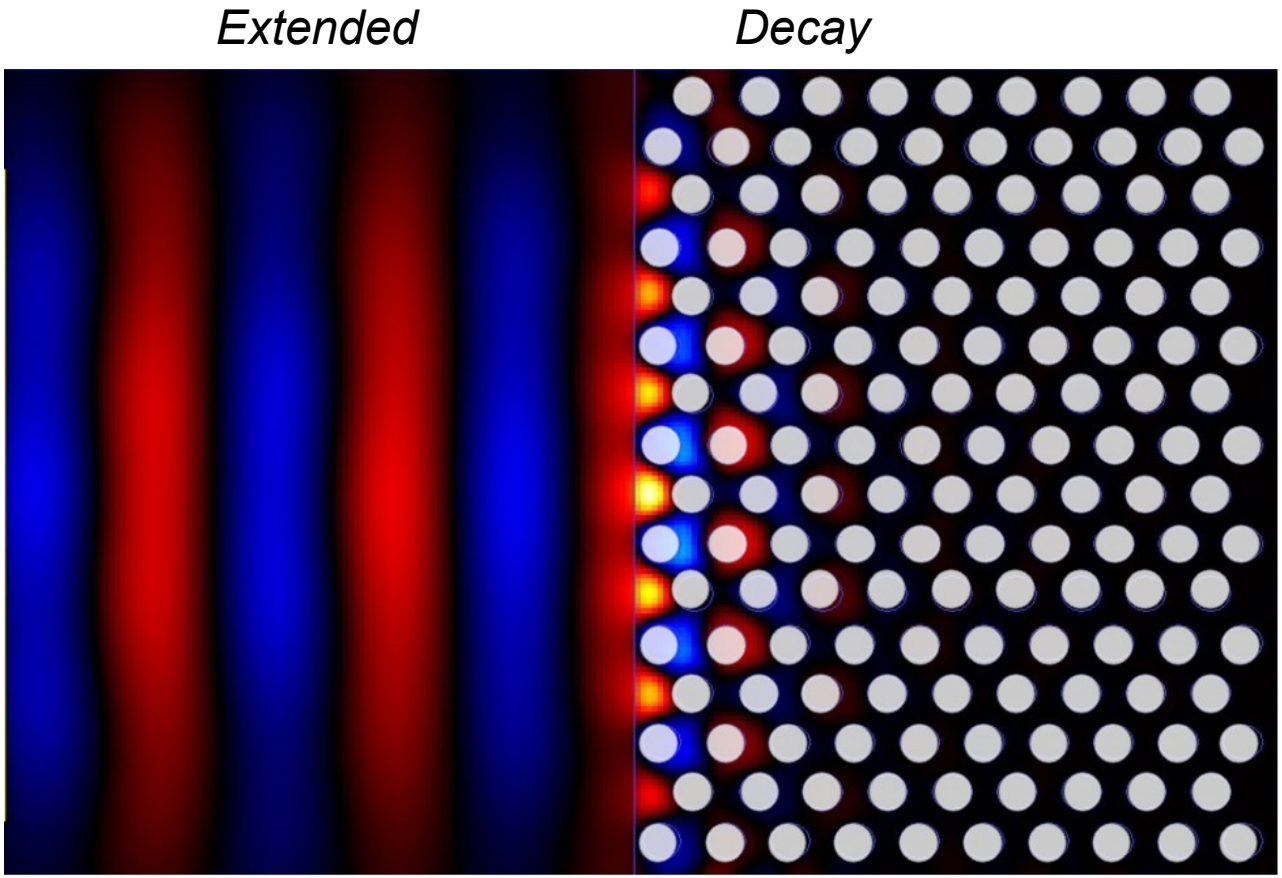

No propagation for frequency in the gap.
External light is totally reflected

Stati nel PGB (ED)

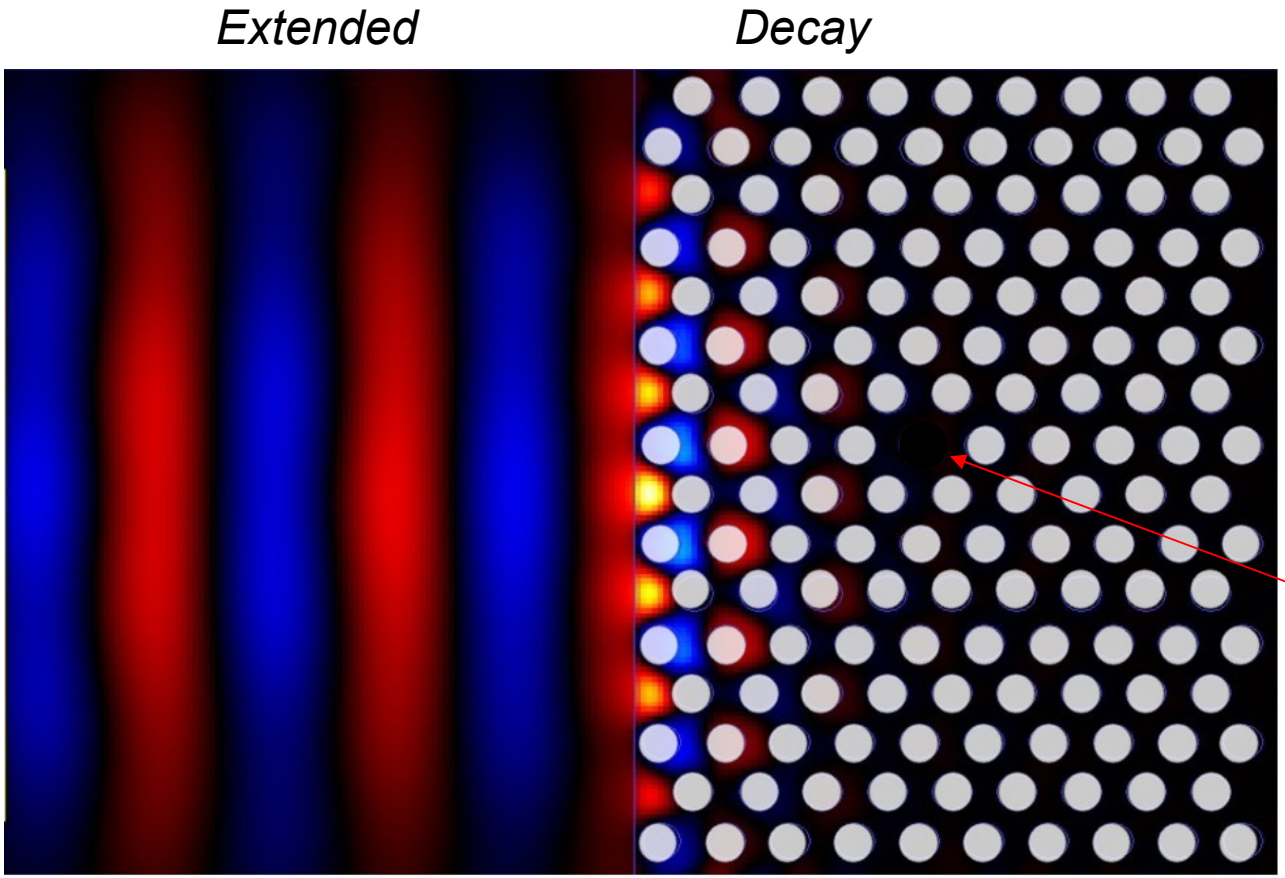

For most frequency nothing happens

Point defect

No propagation for frequency in the gap.
External light is totally reflected

Stati nel PGB (ED)

Extended *Decay*

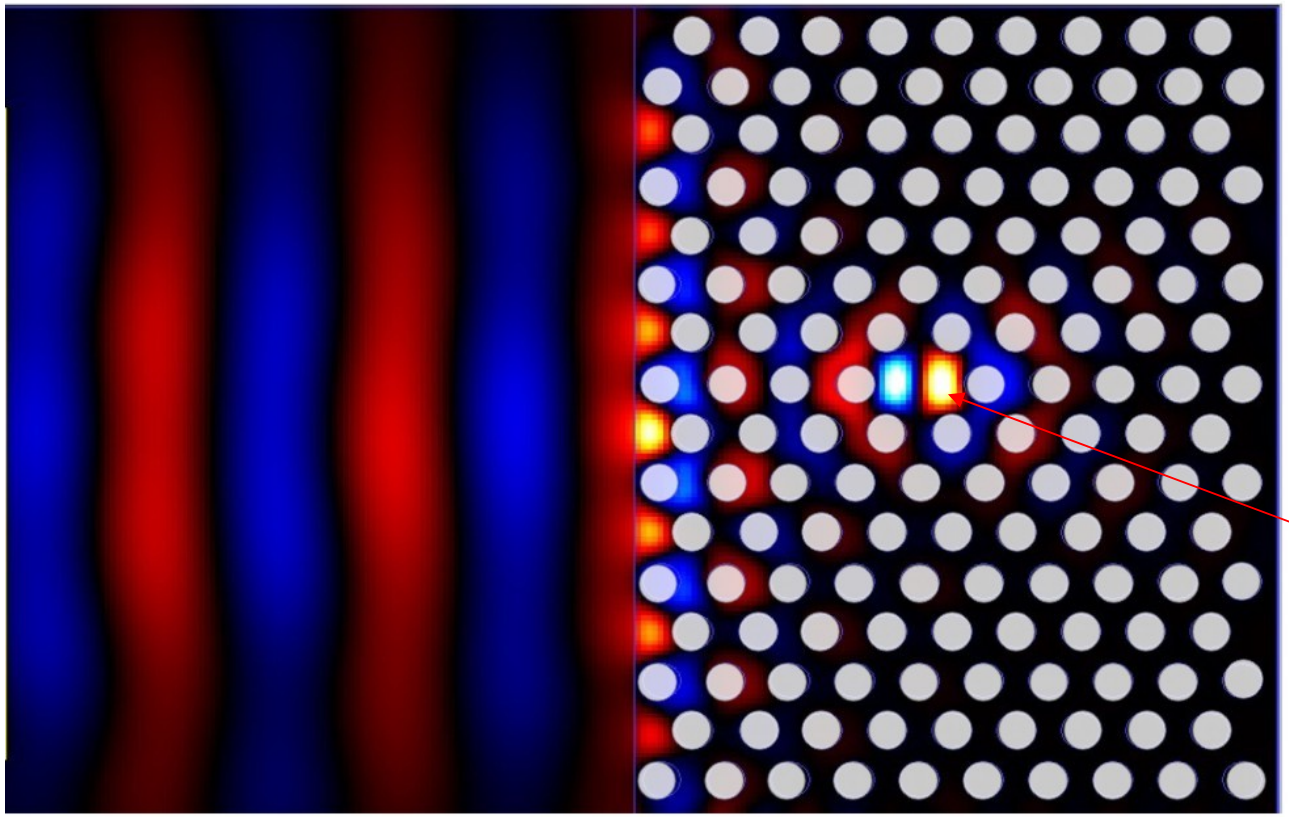

For a given frequency localization occurs

Point defect (DD)

Light localization (with finite lifetime!) around the defect

Spiegazione intuitiva

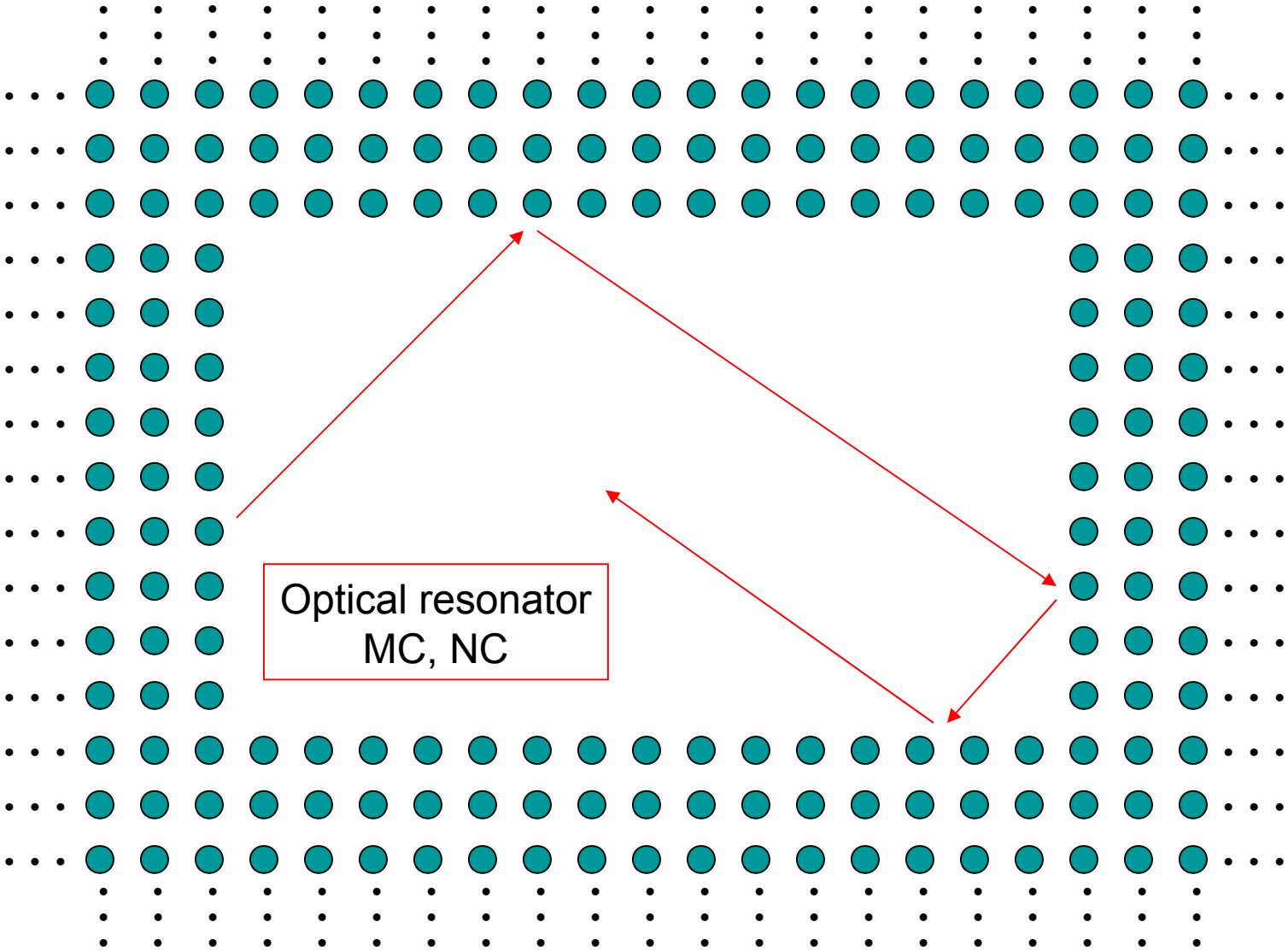

Metodo perturbativo

$$\Delta\omega_n = -\frac{\omega_n}{2}\frac{\int d^3r\vec{E}_n^{\,*}(\vec{r})\delta\varepsilon(\vec{r})\vec{E}_n(\vec{r})}{\int d^3r\vec{E}_n^{\,*}(\vec{r})\varepsilon(\vec{r})\vec{E}_n(\vec{r})}$$

Un aumento di dielettrico produce un red shift
Una diminuzione di dielettrico produce un blue shift

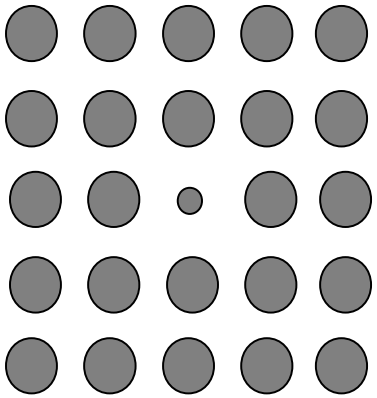

Blue shift

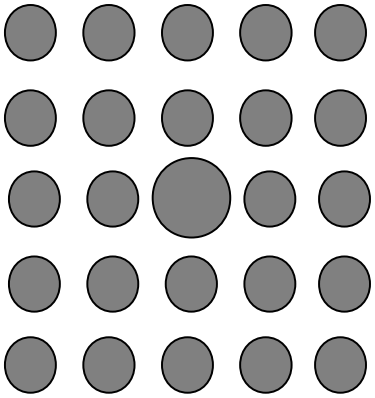

Red shift

Frequenza stato di difetto

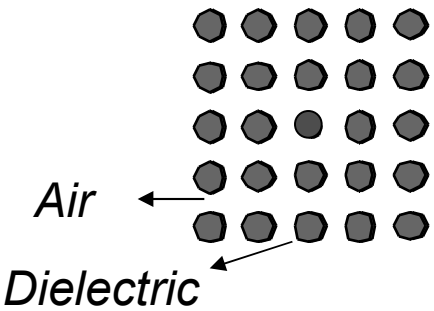

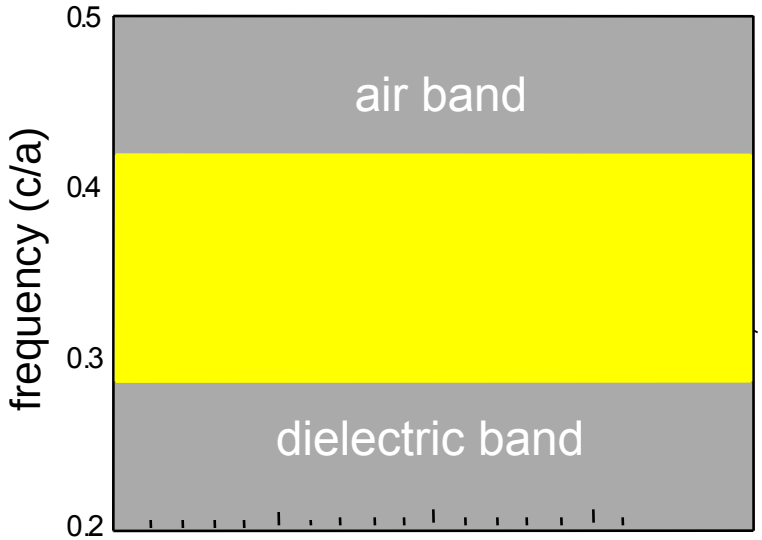

Frequenza stato di difetto

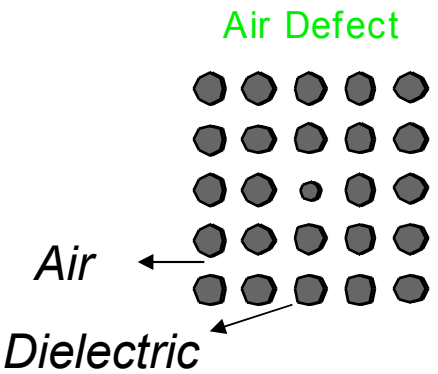

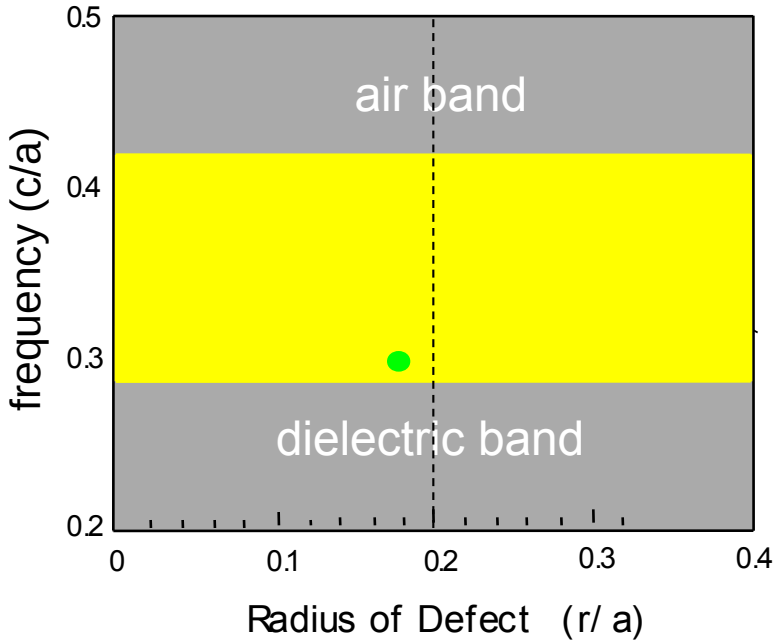

Frequenza stato di difetto

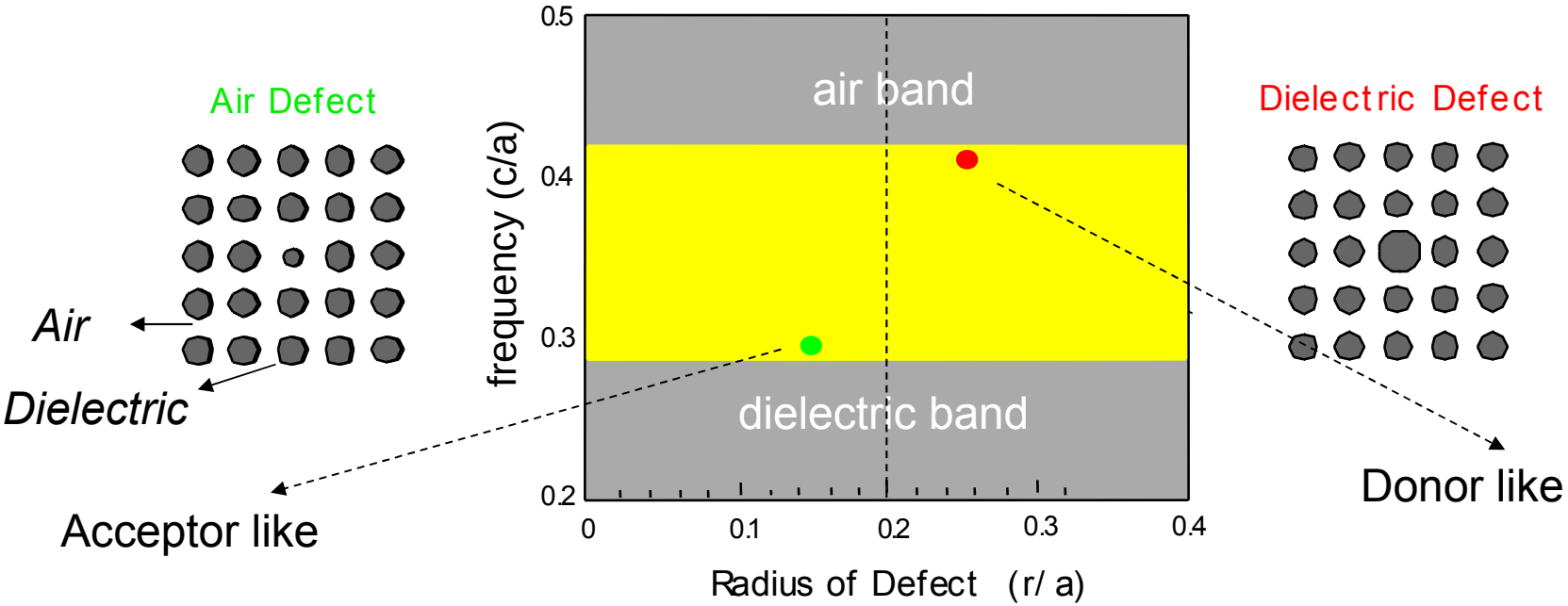

Frequenza stato di difetto

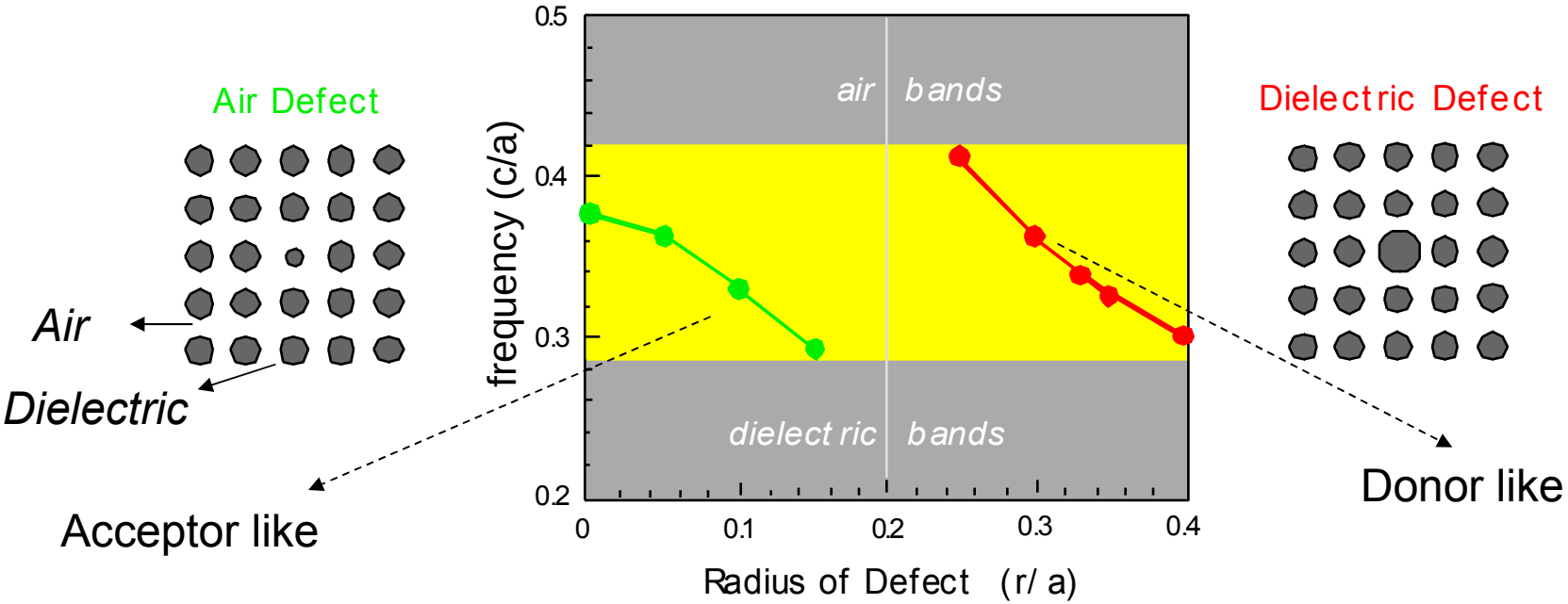

A reader familiar with semiconductor physics can understand this result by analogy with impurities in semiconductors. In that case, atomic impurities create localized electronic states in the band gap of a semiconductor (see, e.g., Pantelides, 1978). Attractive potentials create a state at the conduction band edge, and repulsive potentials create a state at the valence band edge. In the photonic case, we can put the defect mode within the band gap with a suitable choice of $\varepsilon_{\text{defect}}$.

Increasing the dielectric function is analogous to increase the attractive potential (D)
Decreasing the dielectric function is analogous to decrease the attractive potential (A)

Distribuzione stato di difetto

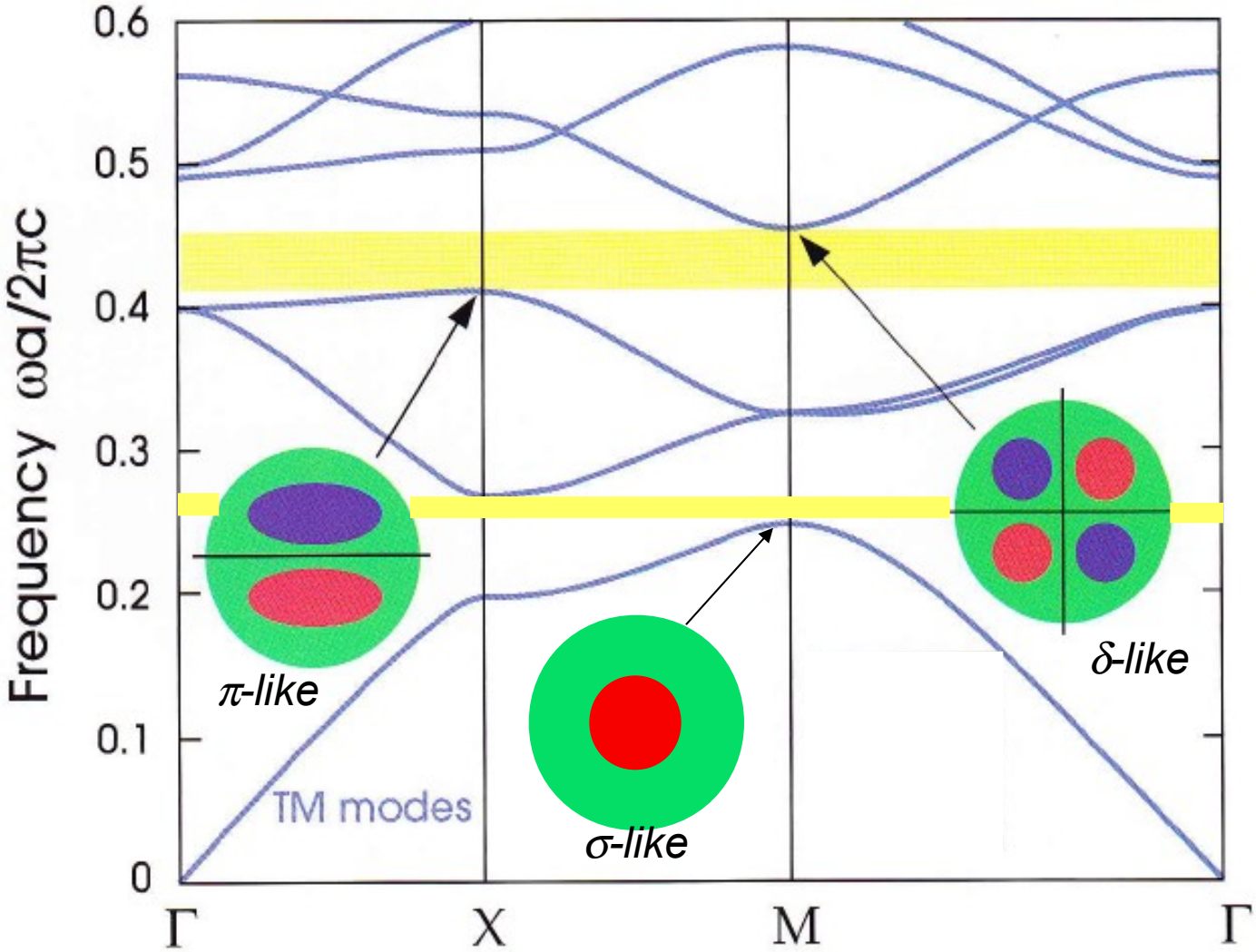

Distribuzione stato di difetto

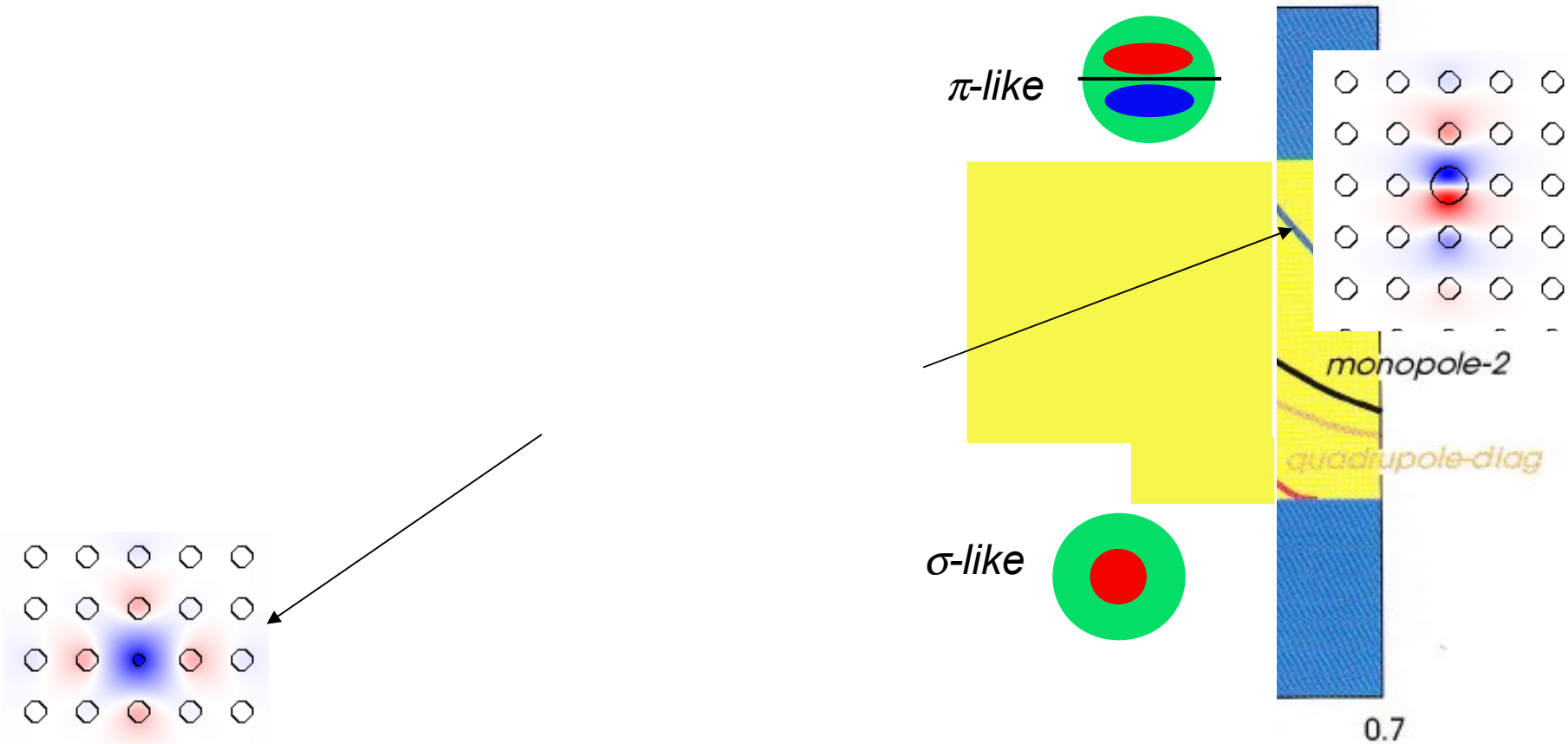

Figure 16: The evolution of localized modes associated with a defect column in an otherw
perfect square lattice with the parameters of figure 2, as the defect's *radius* is changed. A

Distribuzione stato di difetto

Figure 16: The evolution of localized modes associated with a defect column in an otherwise perfect square lattice with the parameters of figure 2, as the defect's *radius* is changed. A

Distribuzione stato di difetto

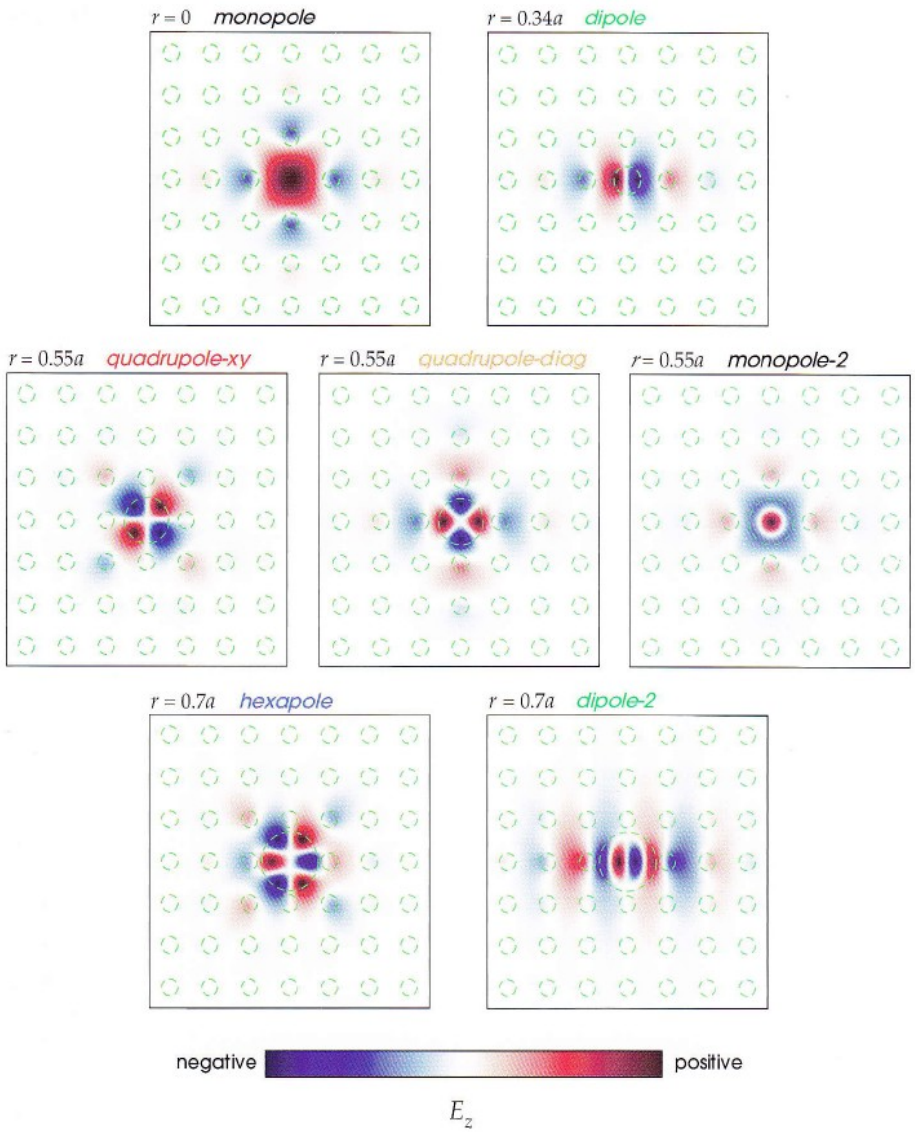

Distribuzione stato di difetto

La simmetria del reticolo e del difetto definiscono sia la distribuzione del modo che le eventuali degenerazioni

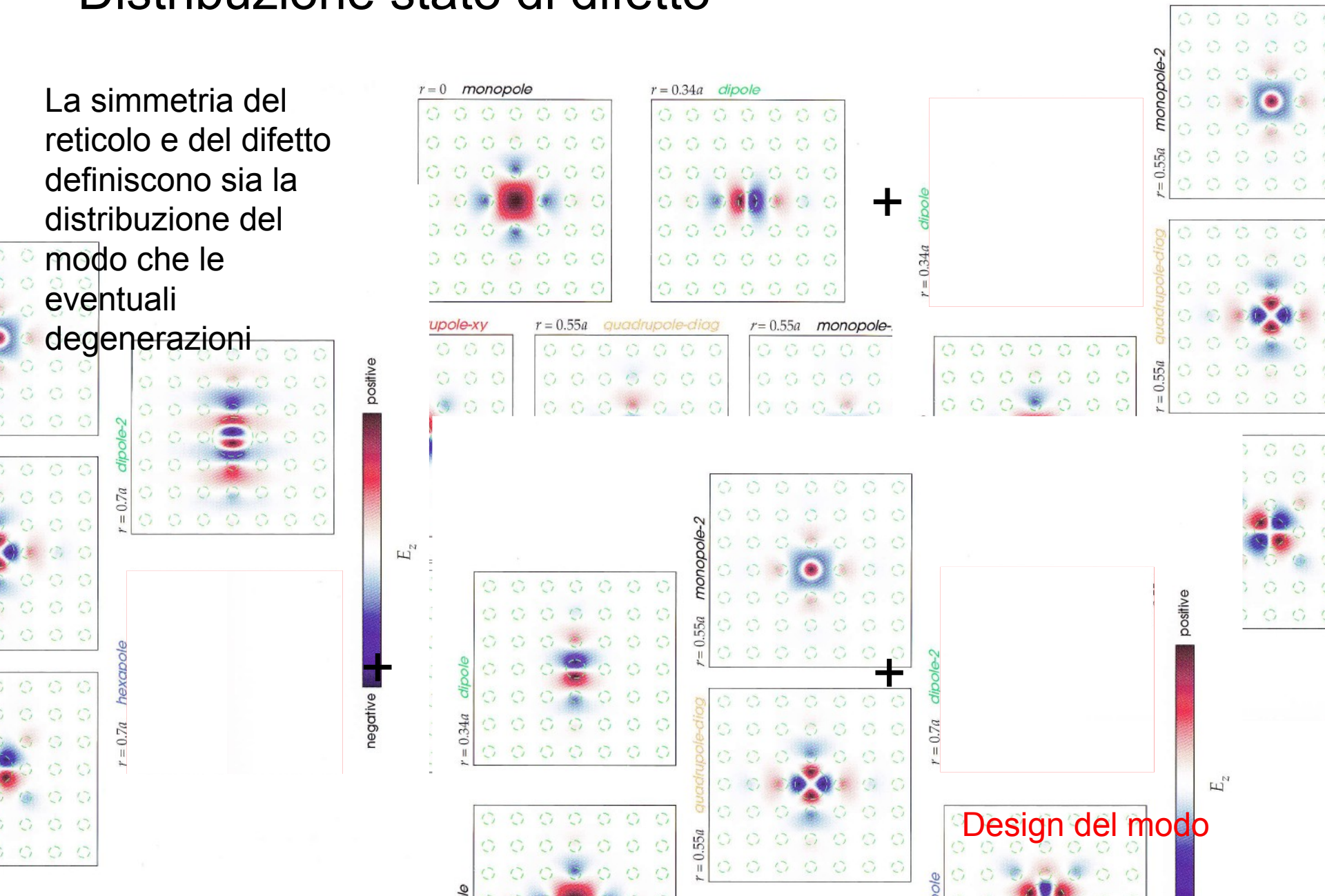

Design del modo

Difetto di linea

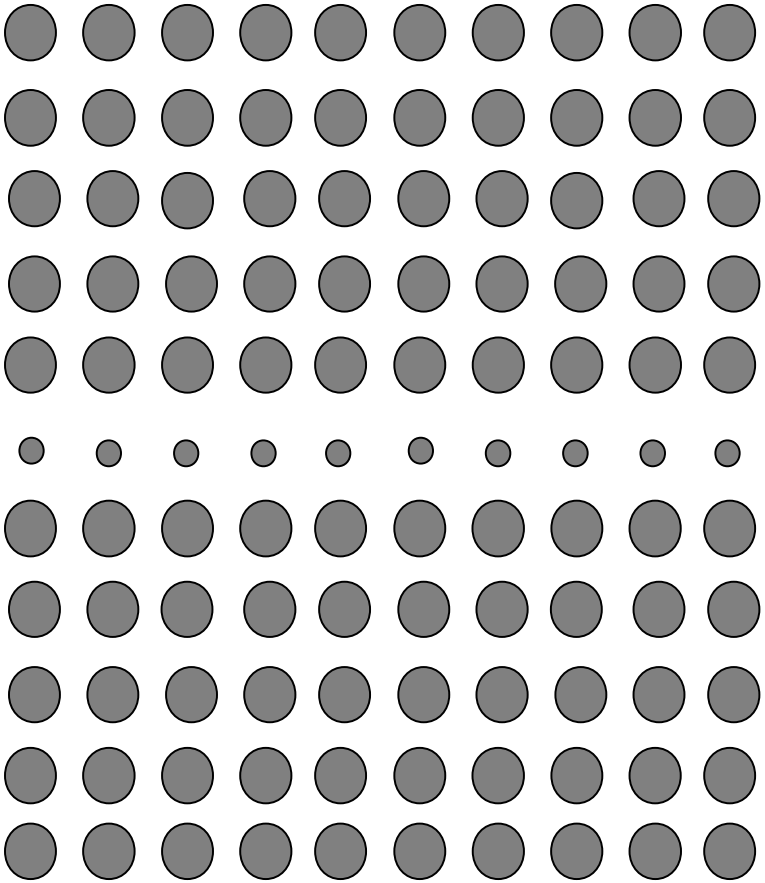

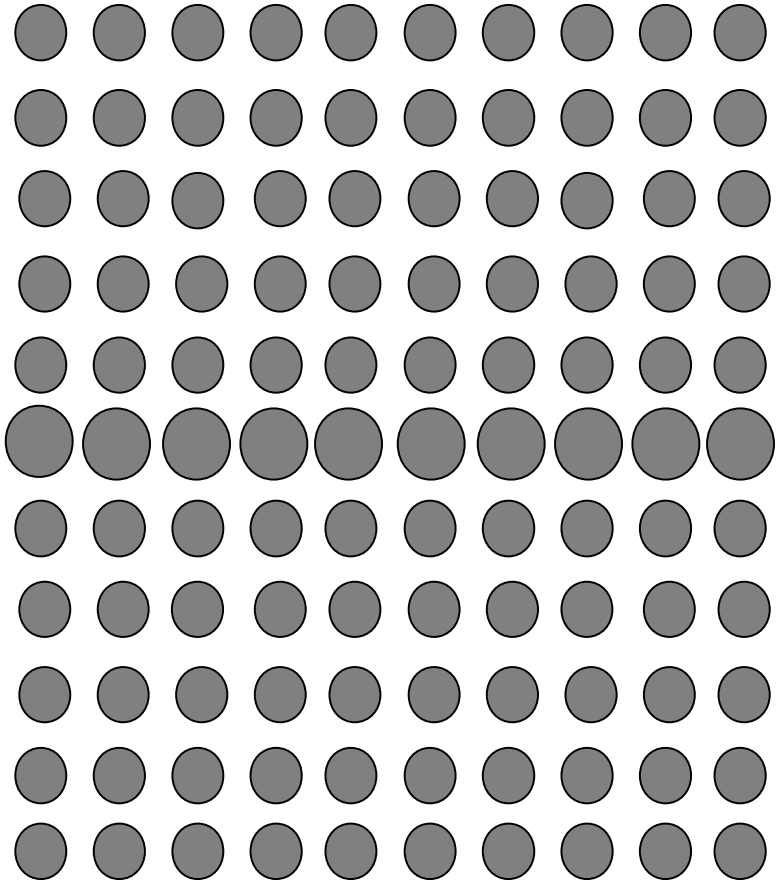

Difetto di linea

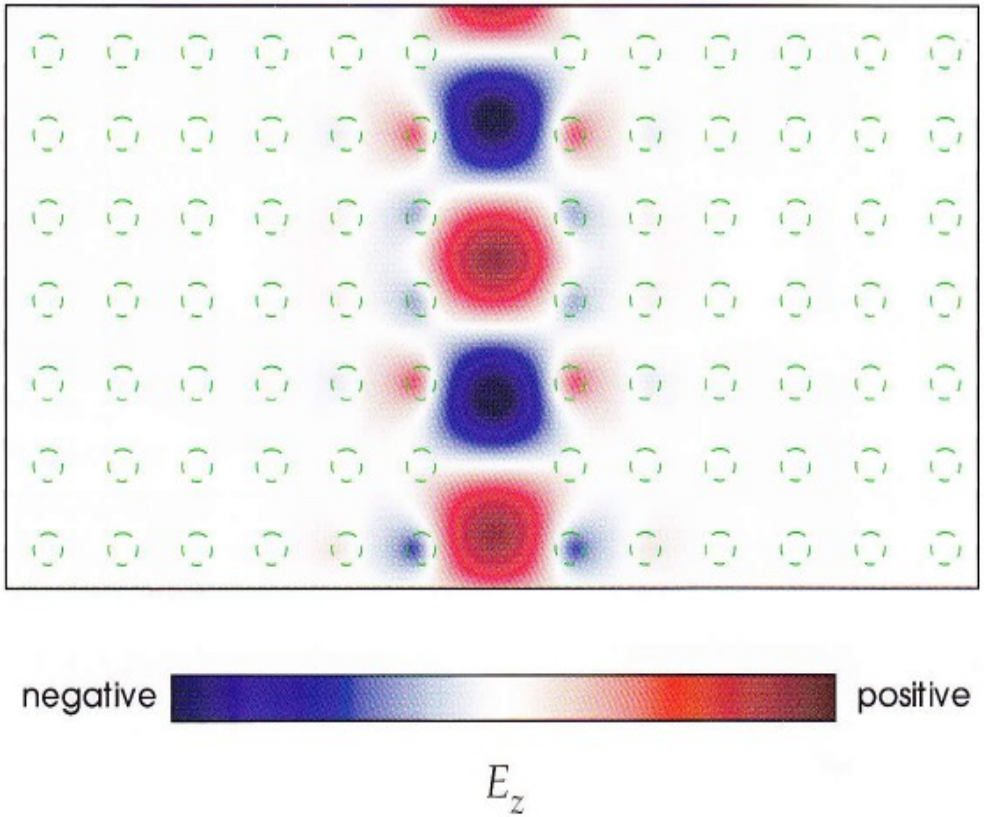

Figure 18: Electric-field (E_z) pattern associated with a linear defect formed by removing a column of rods from an otherwise-perfect square lattice of rods in air. The resulting field, shown here for a wave vector $k_y = 0.3\,(2\pi/a)$ along the defect, is a **waveguide mode** propagating along the defect. The rods are shown as dashed green outlines.

Difetto di linea: guida d'onda

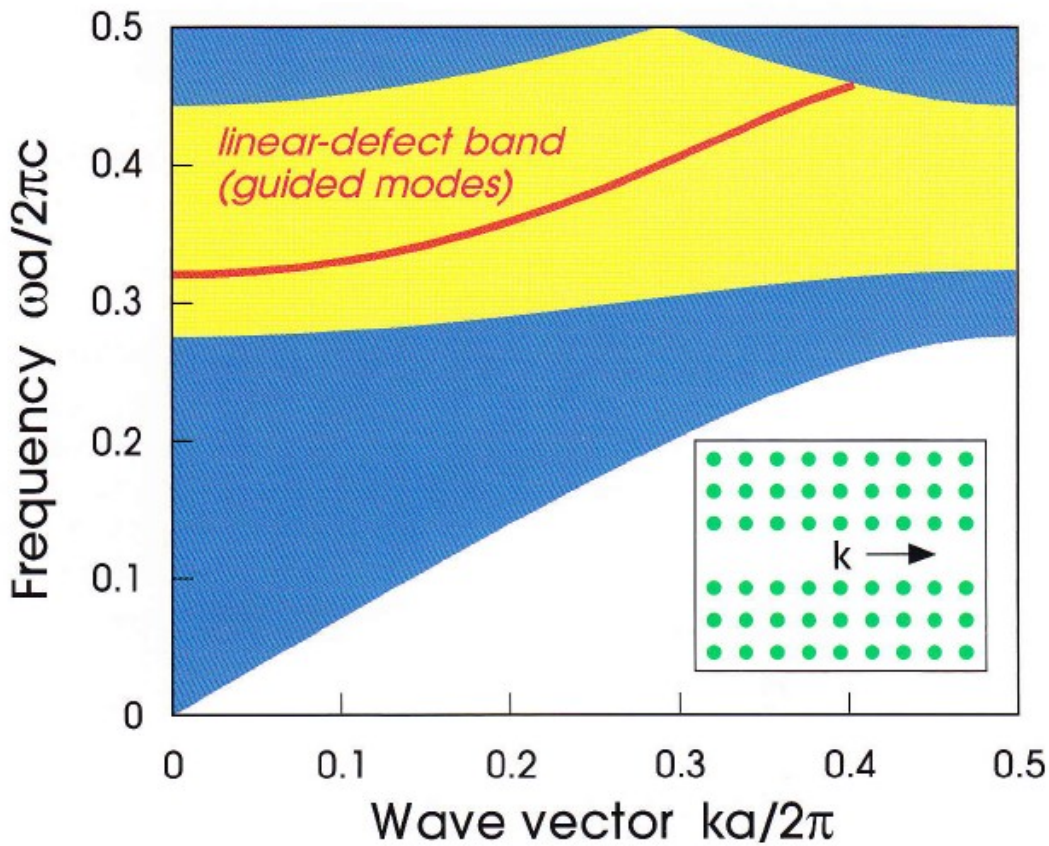

Figure 19: The projected band structure of the line defect (inset) formed by removing a row (or column) of rods from an otherwise perfect square lattice from figure 2, plotted versus the wave vector component k along the defect. The extended modes in the crystal become continuum regions (blue), whereas inside the band gap (yellow) a defect band (red) is introduced corresponding to a localized state as in figure 18.

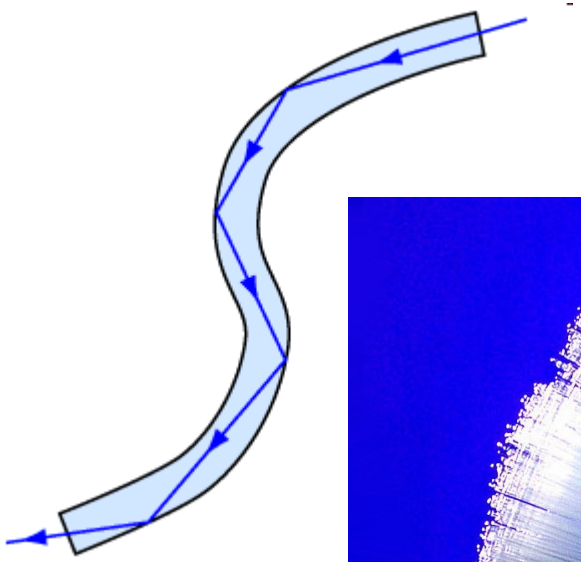

Fibre ottiche

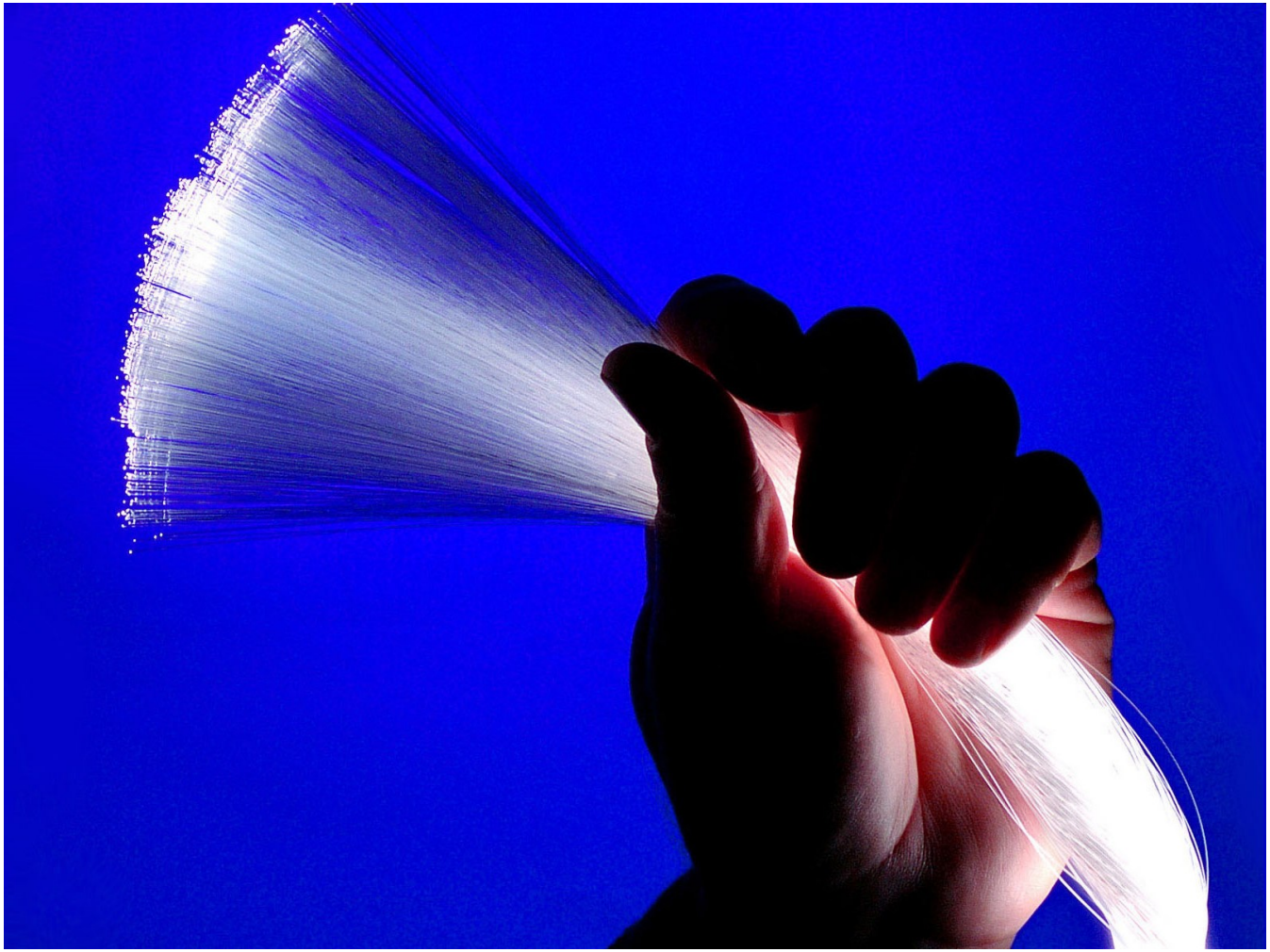

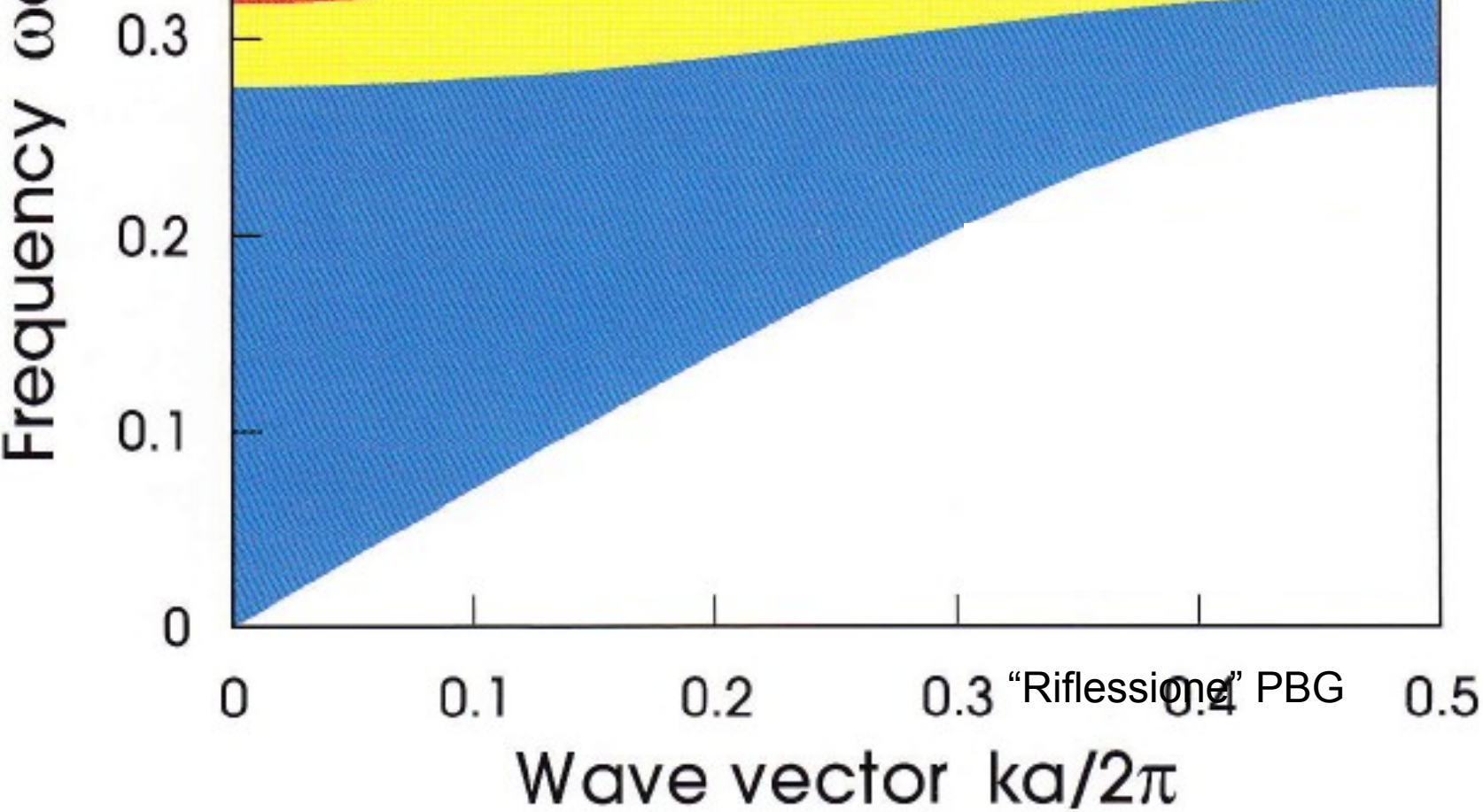

"Riflessione" PBG

9: The projected band structure of the line defect (inset) formed by removing a row
mn) of rods from an otherwise perfect square lattice from figure 2, plotted versus the
ector component k along the defect. The extended modes in the crystal become
um regions (blue), whereas inside the band gap (yellow) a defect band (red) is
ed corresponding to a localized state as in figure 18.

Photonic crystal vs. conventional waveguide

High-index region

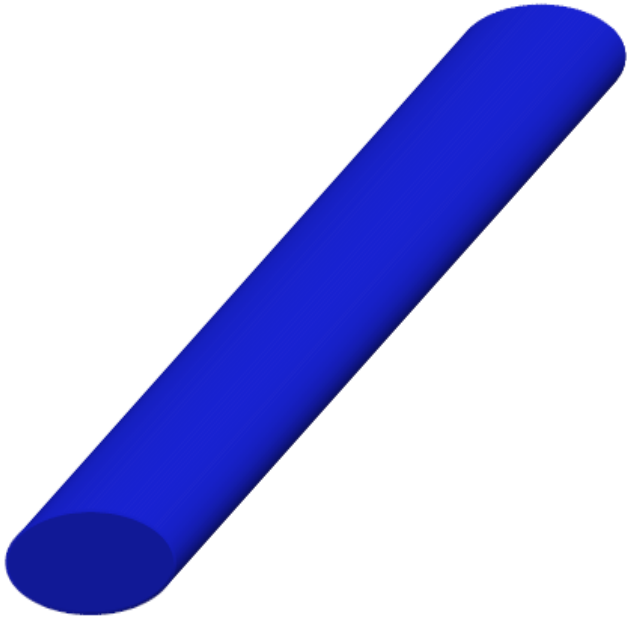

Conventional waveguide

Low index region

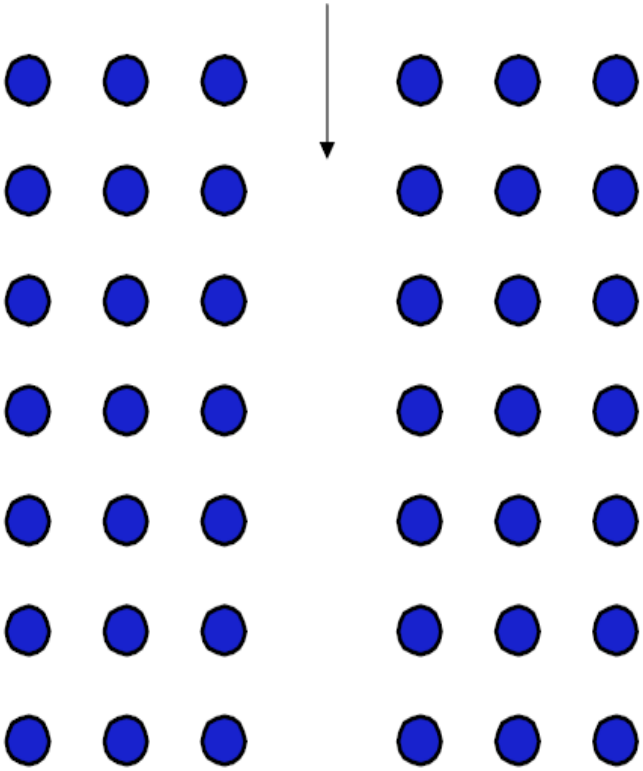

Photonic crystal waveguide

Riflessione totale: implica limite curvatura massima

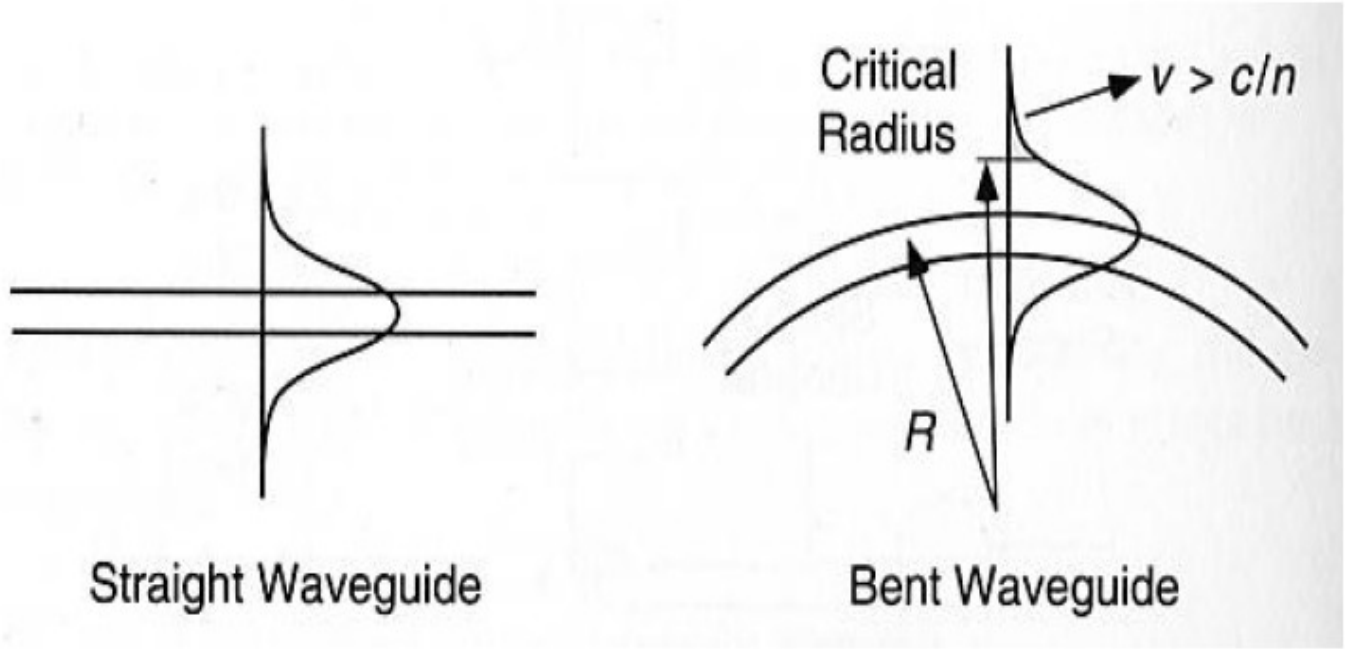

Riflessione PGB: no limite curvatura massima

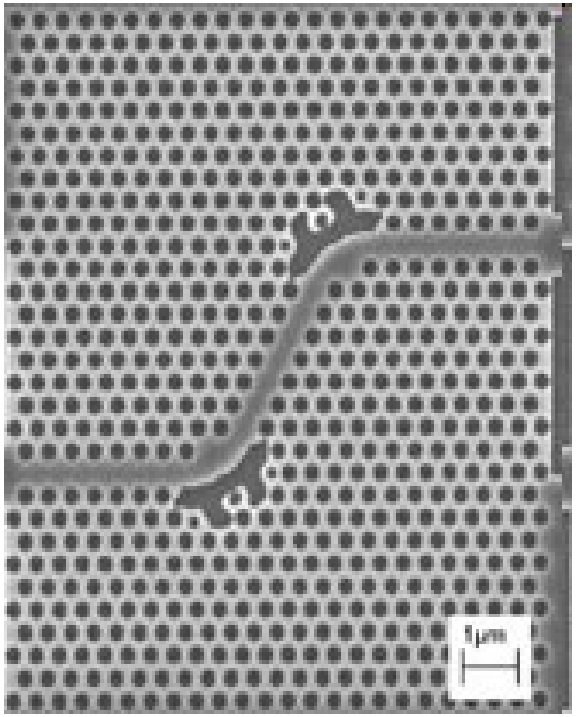

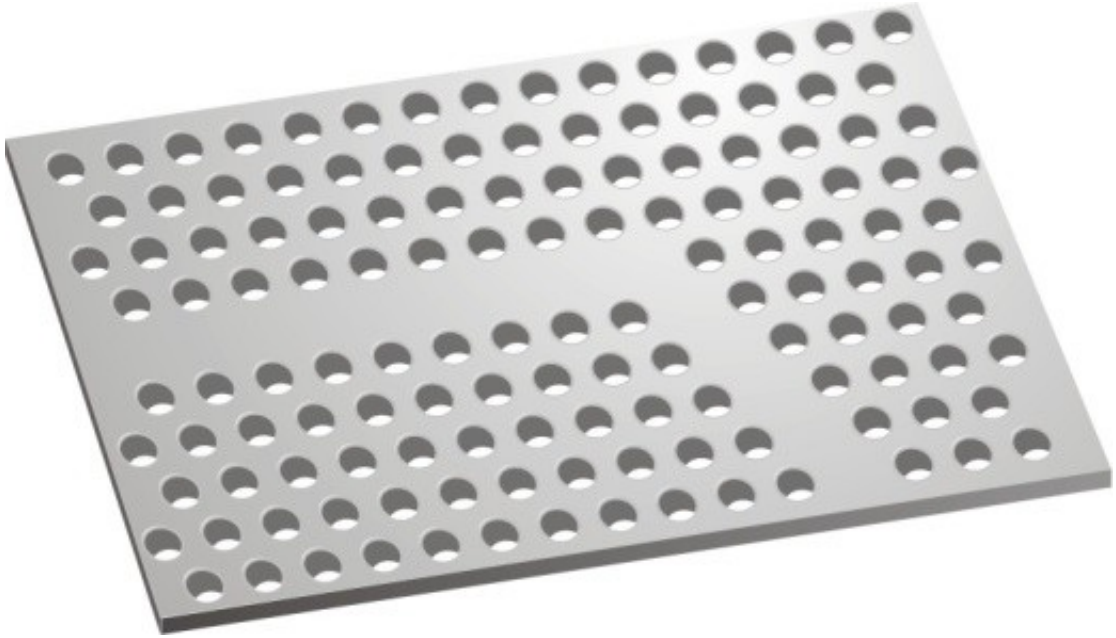

L-Shaped

T-Shaped

Riflessione PGB a 90°

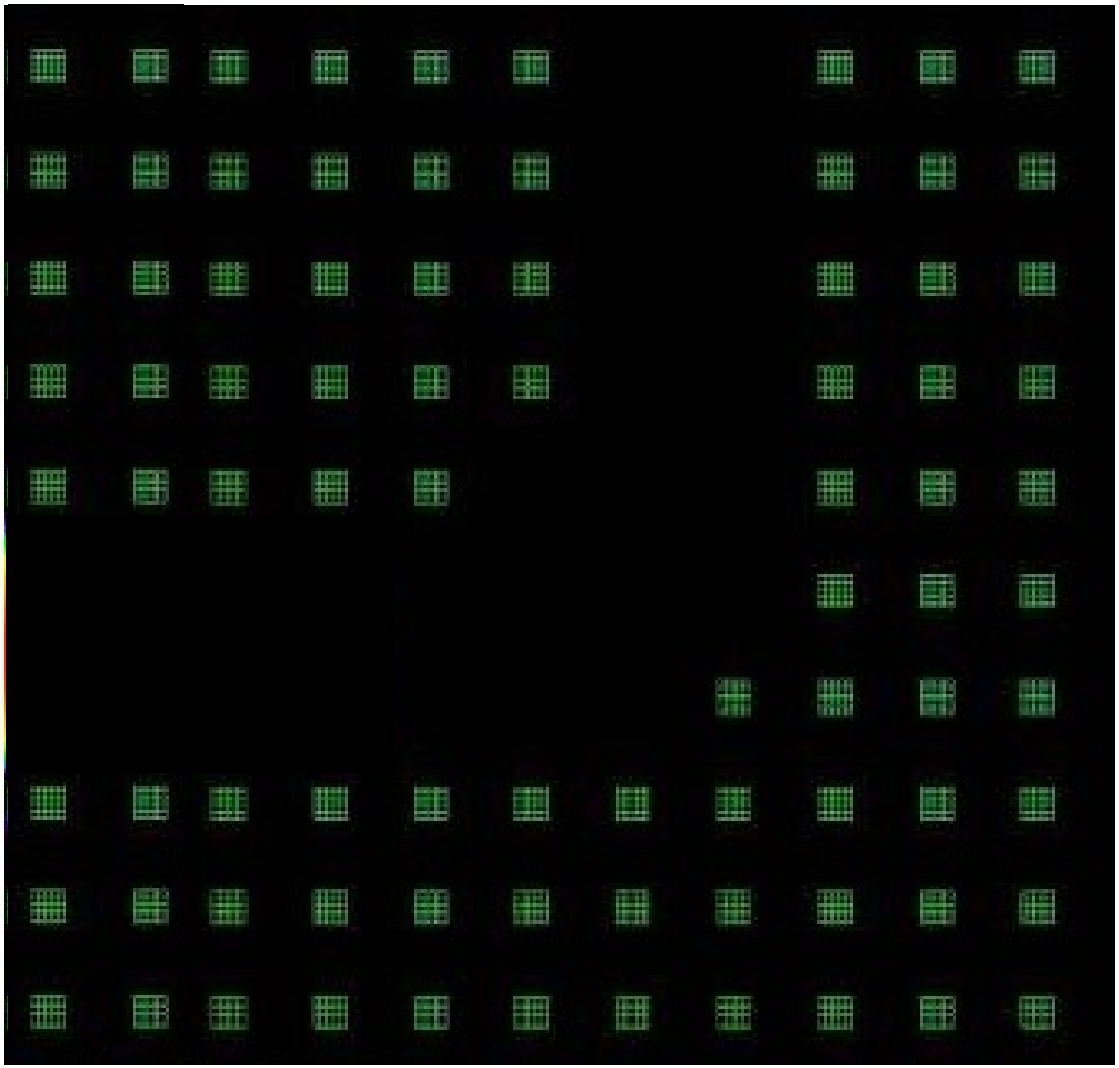

Riflessione PGB a 90°

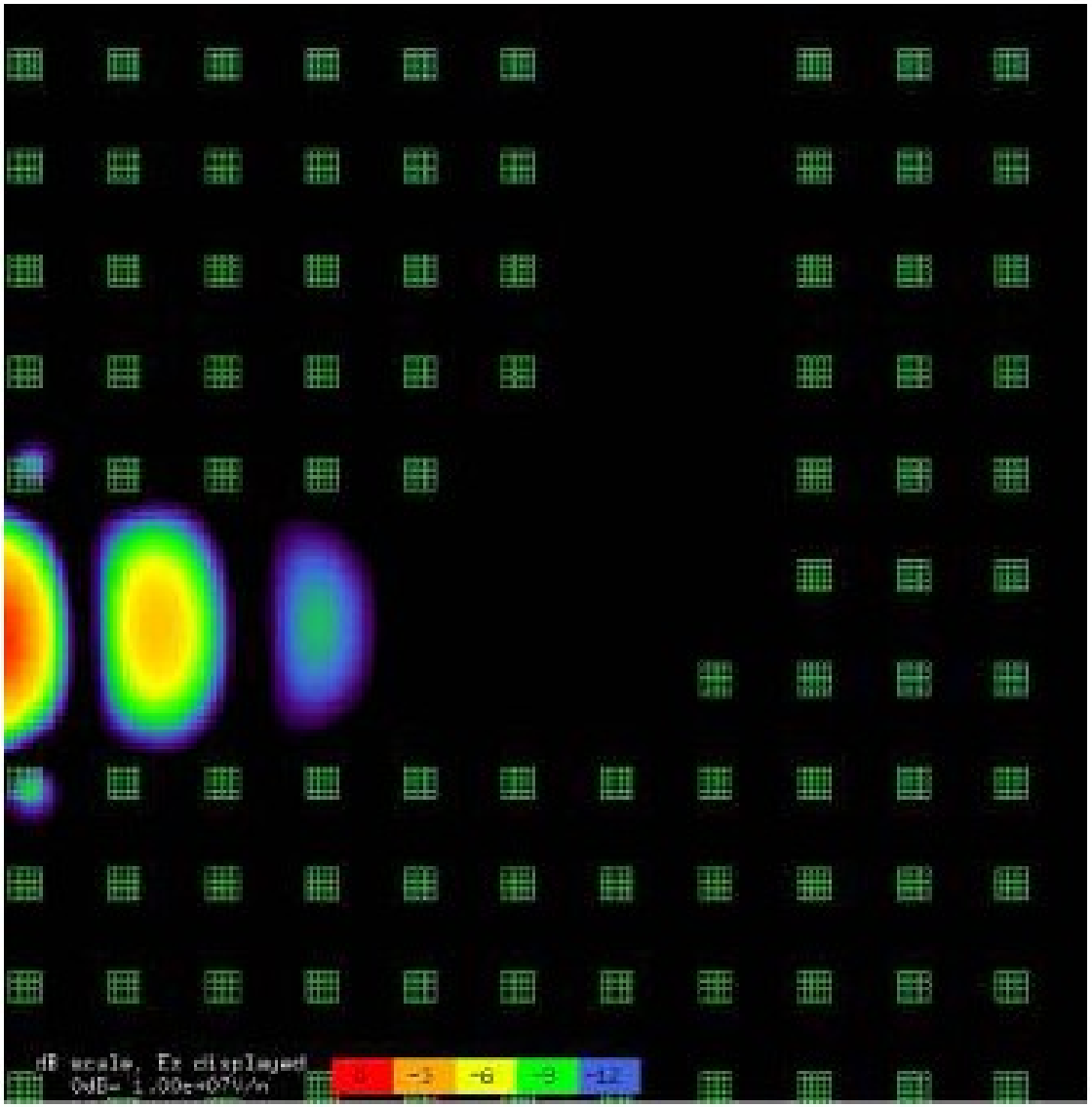

Riflessione PGB a 90°

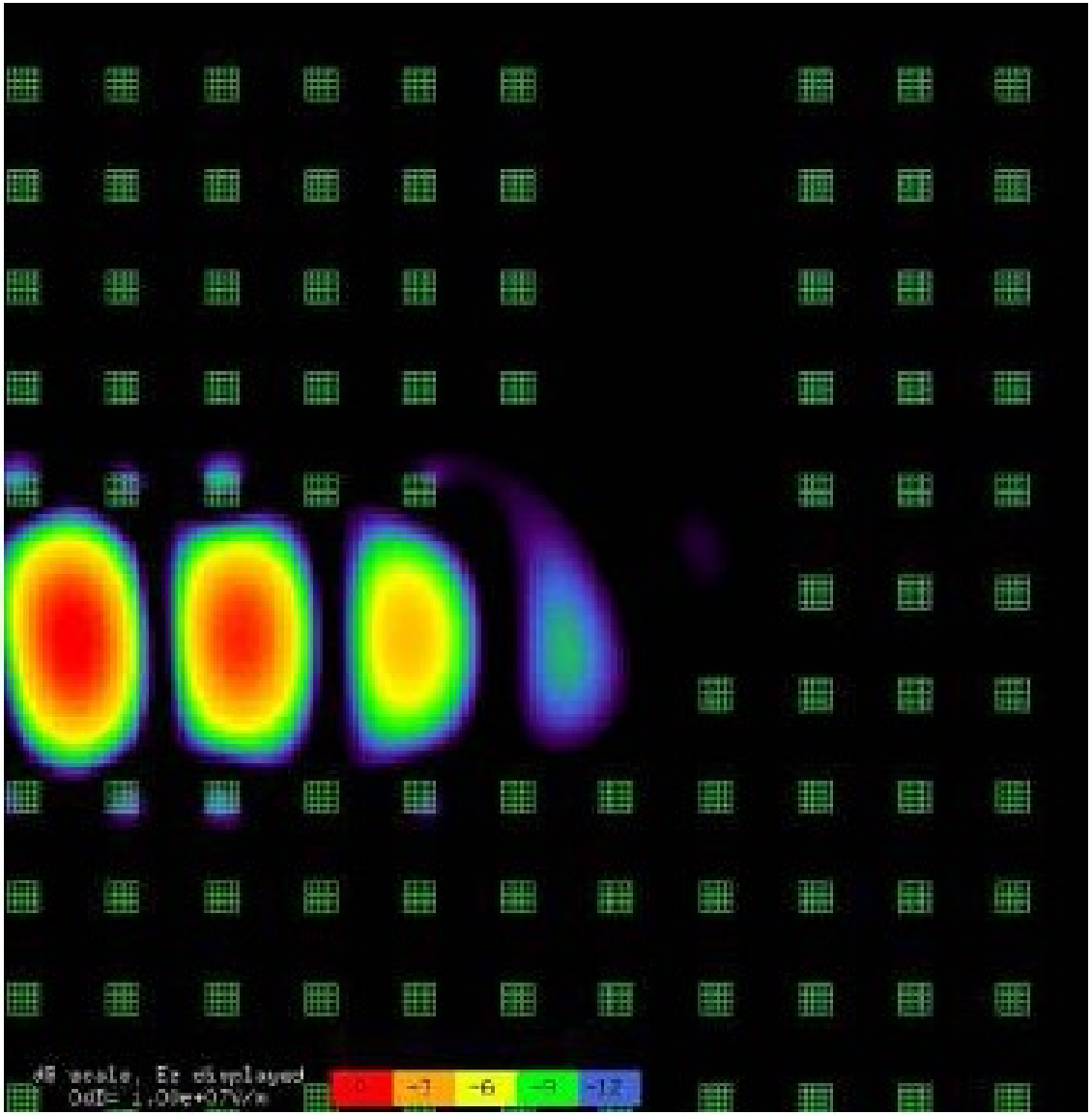

Riflessione PGB a 90°

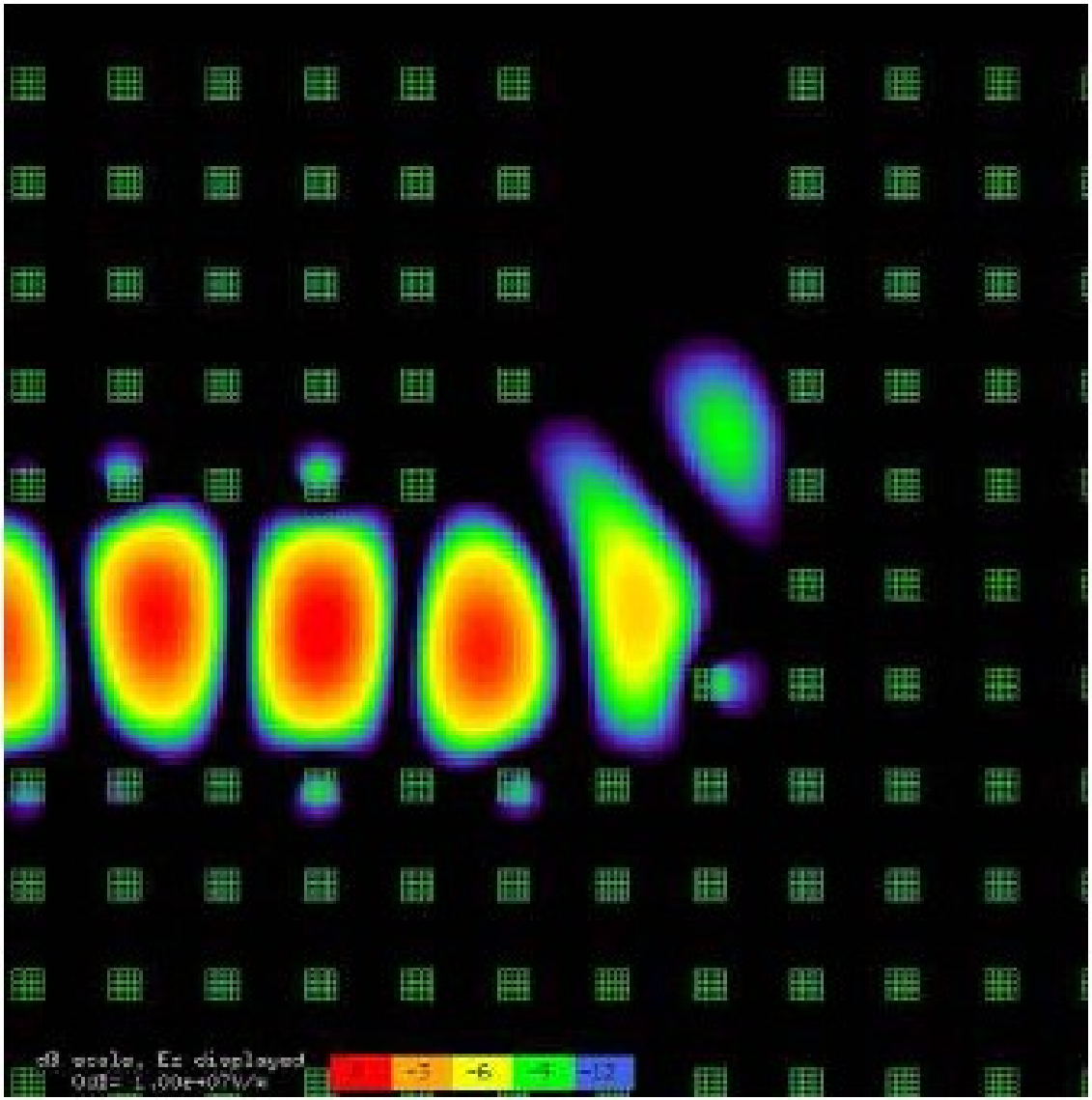

Riflessione PGB a 90°

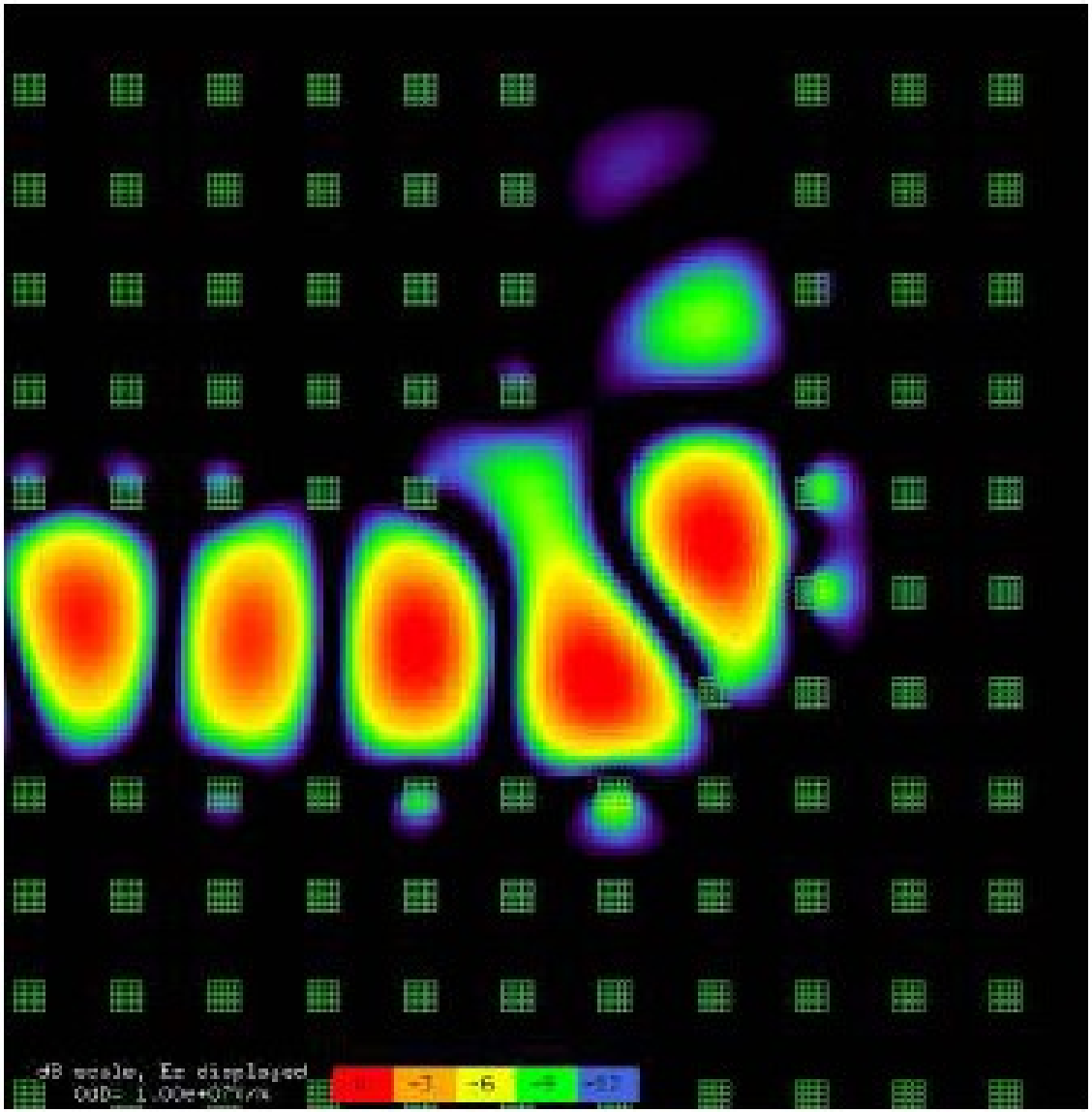

Riflessione PGB a 90°

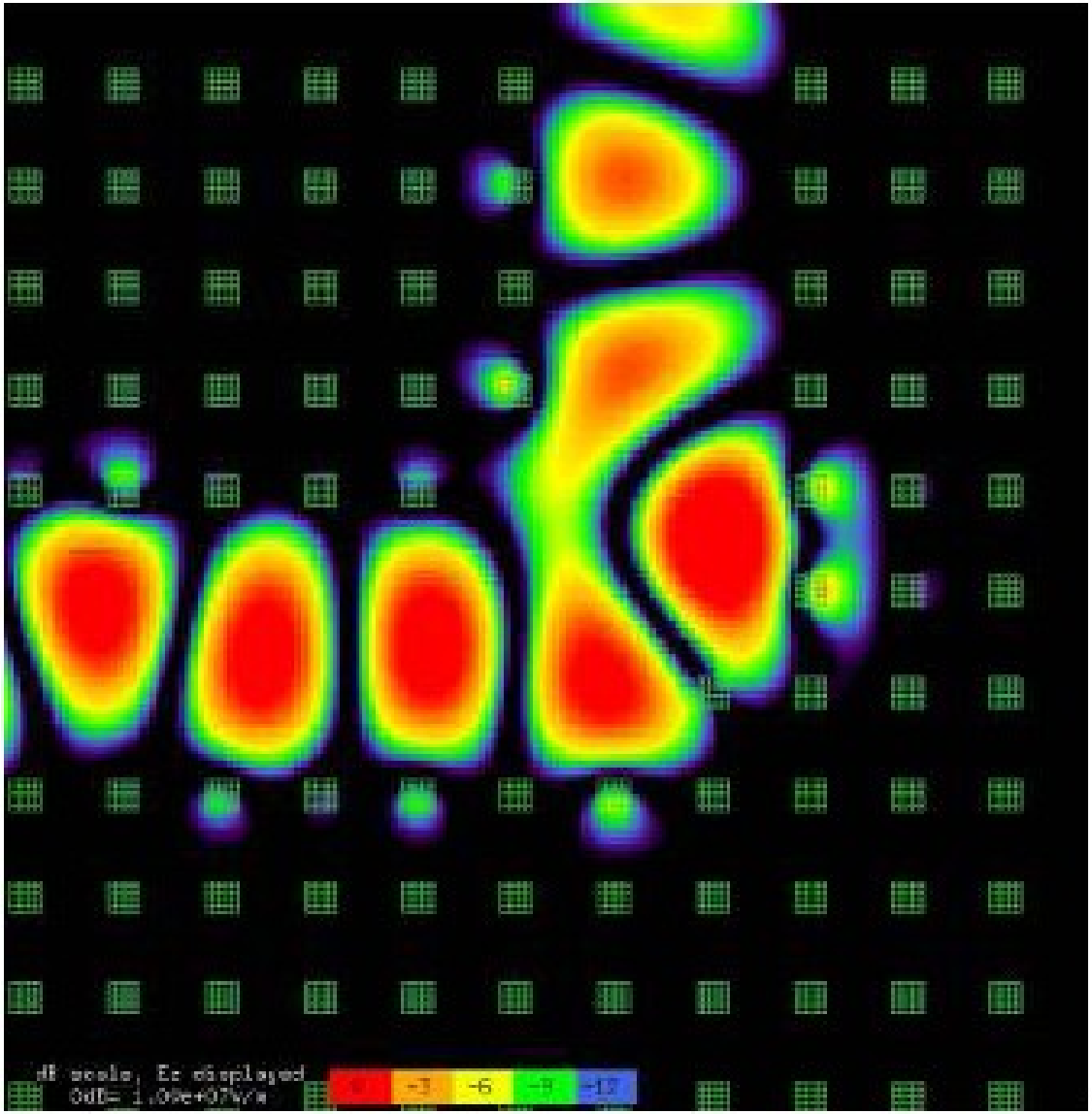

Fotonica 2D
Molti gradi di libertà

Nano-Infiltrazione di liquidi

APPLIED PHYSICS LETTERS 89, 211117 (2006)

Rewritable photonic circuits

Francesca Intonti,[a] Silvia Vignolini, Volker Türck, and Marcello Colocci
European Laboratory for Non-Linear Spectroscopy, via N. Carrara 1, Sesto Fiorentino, Firenze, 50019 Italy

Pipette's tip diameter 500nm

ZOOM

SETUP

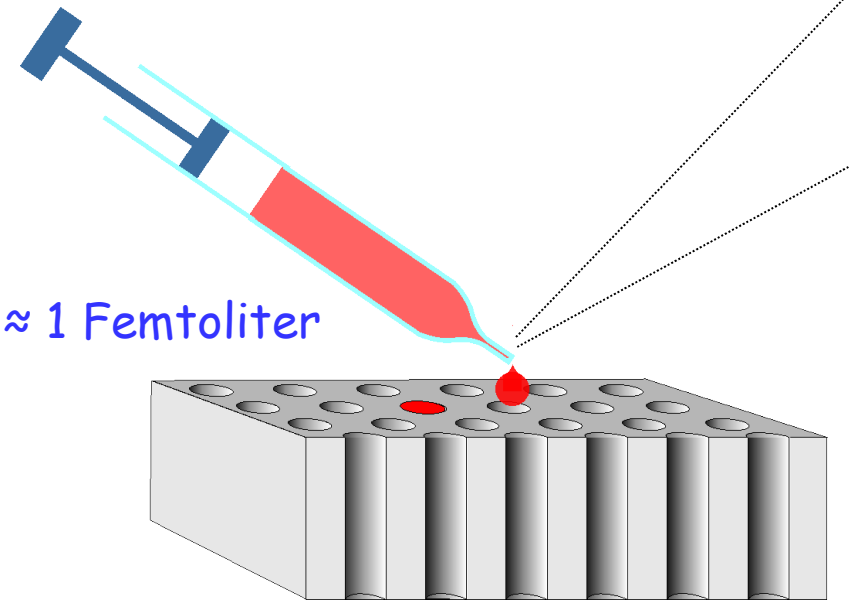

≈ 1 Femtoliter

Hydraulical Micro-translator accuracy ≈ 100 nm

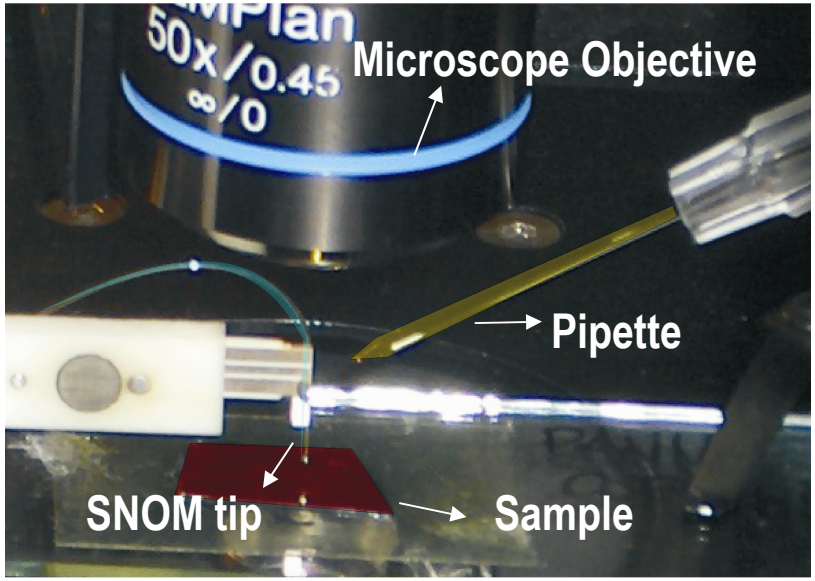

Nano-Infiltrazione di liquidi

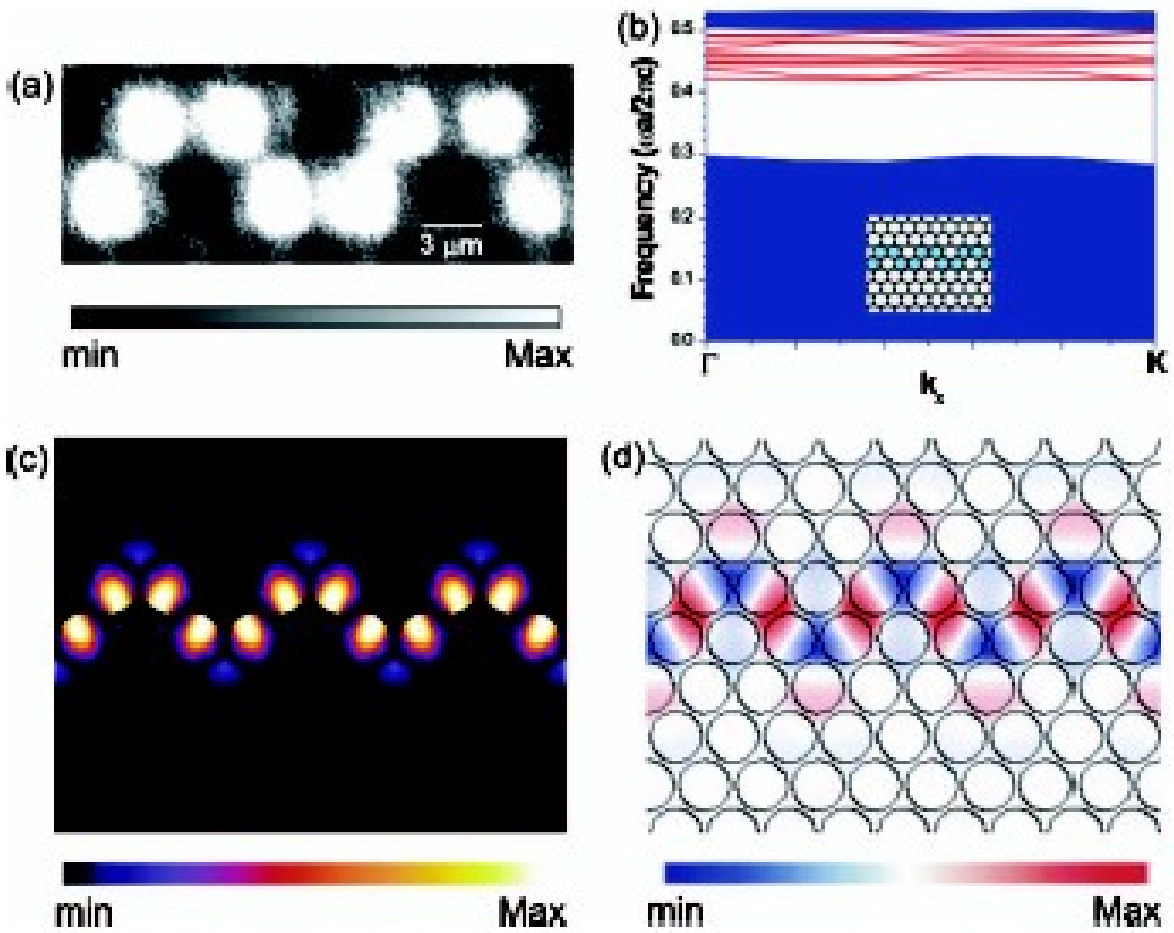

- Guide d’onda di forma arbitraria
- Guide riscrivibili in modo reversibile
- Indroduzione di emettitori o LC

Optical Multiplexer

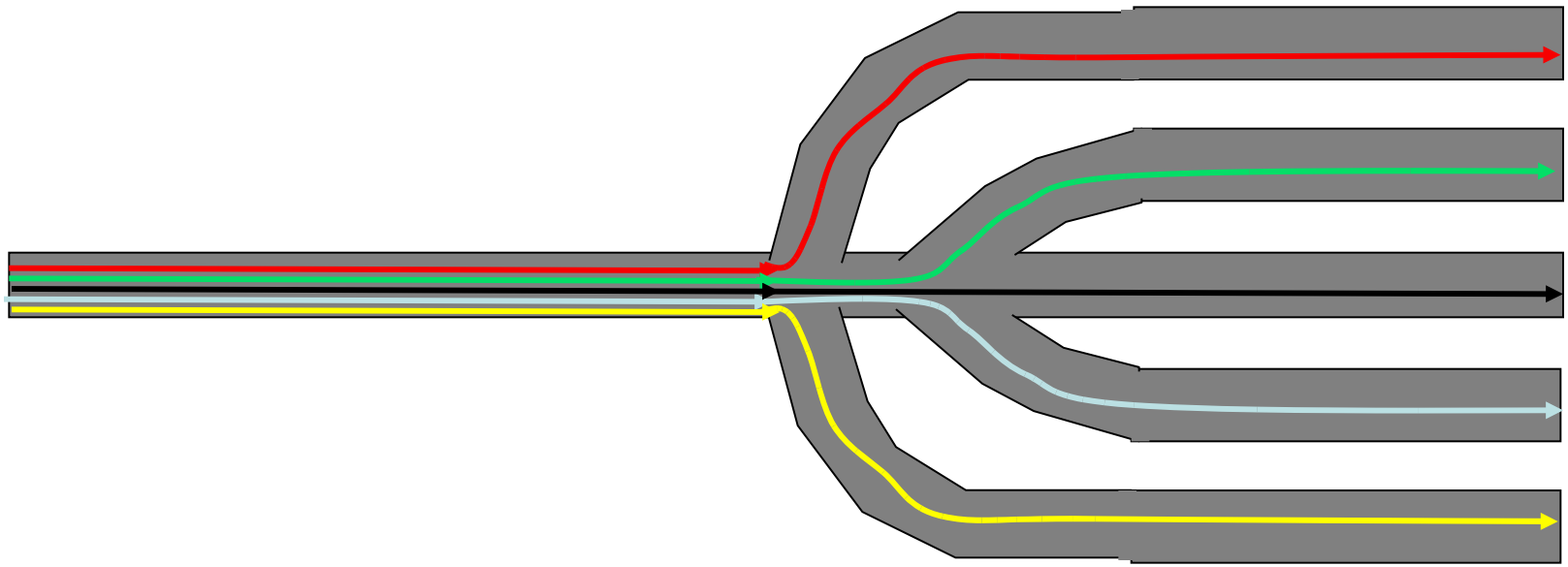

Photonic Multiplexer

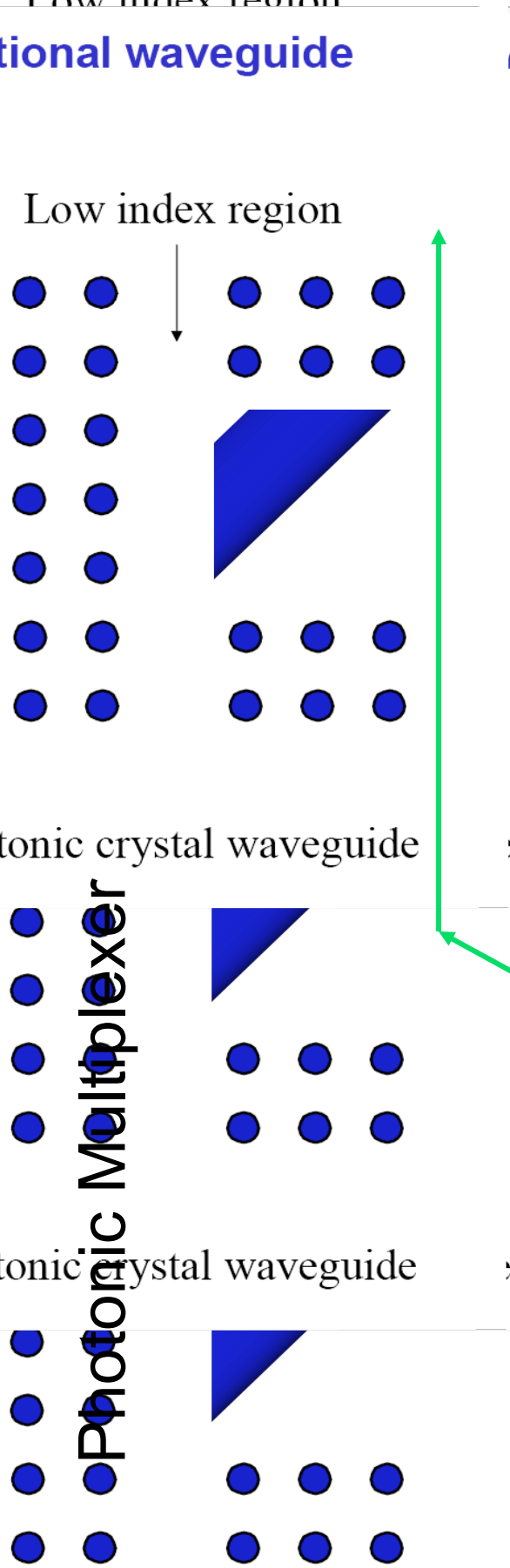

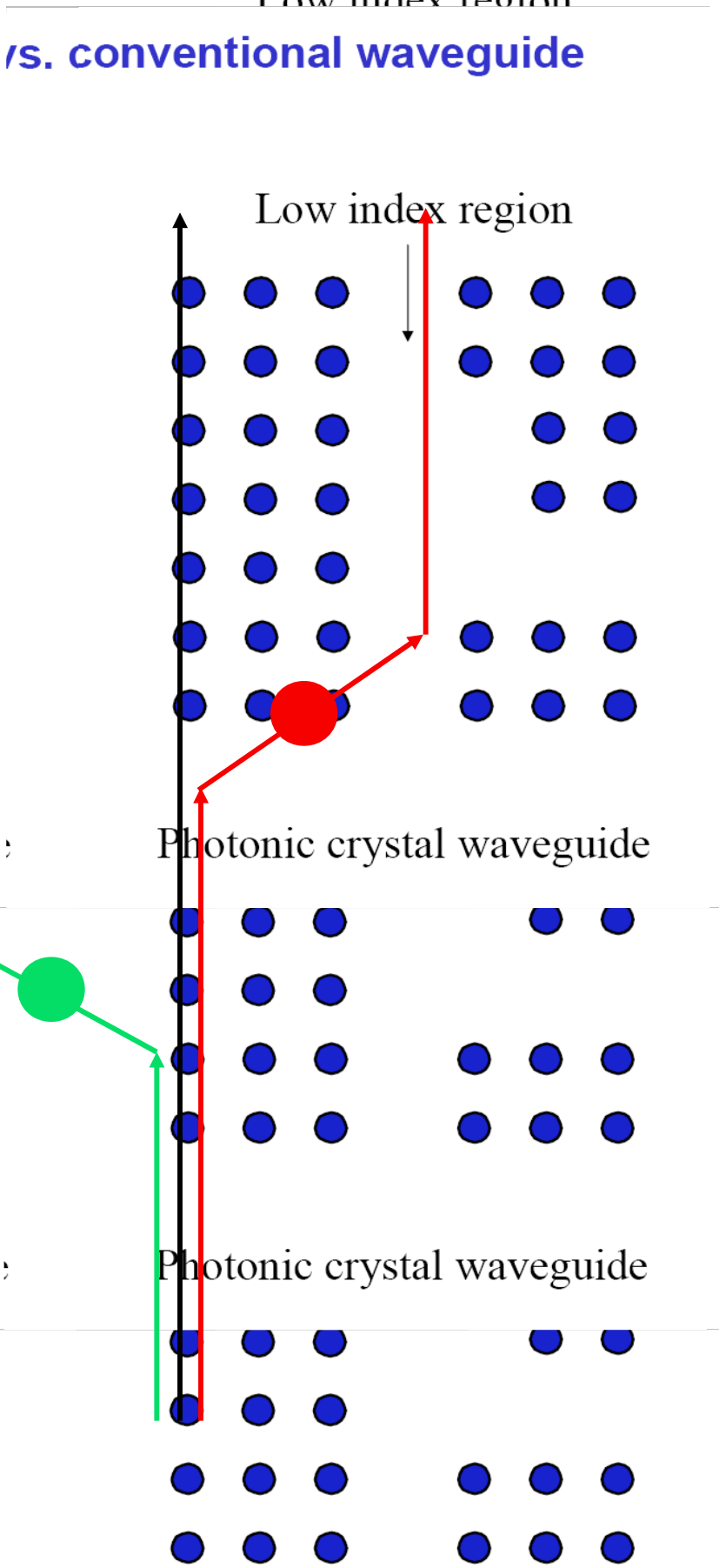

Difetto tunabile: ring resonator

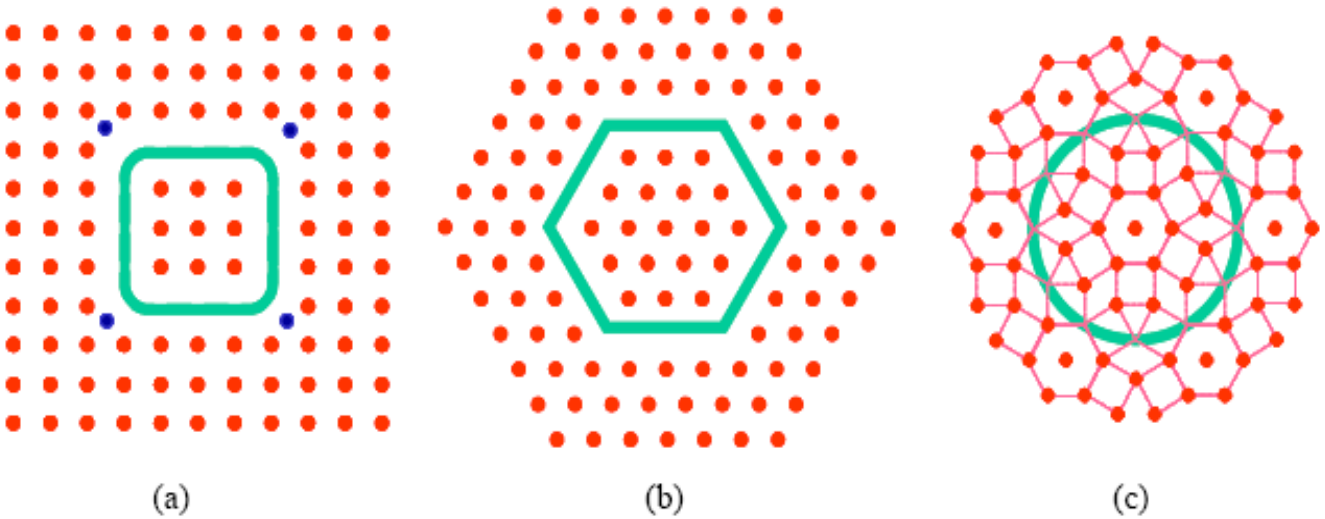

Fig. 1. Photonic crystal ring resonators (PCRRs): (a) Quasi-square ring PCRR in square lattice; (b) Hexagonal ring PCRR in triangular lattice; (c) Circular ring PCRR in quasi-photonic crystal structure (12-fold symmetry as shown).

Difetti grandi hanno multimodi e possibilità di disegnare il loro profilo di campo

Ring resonator

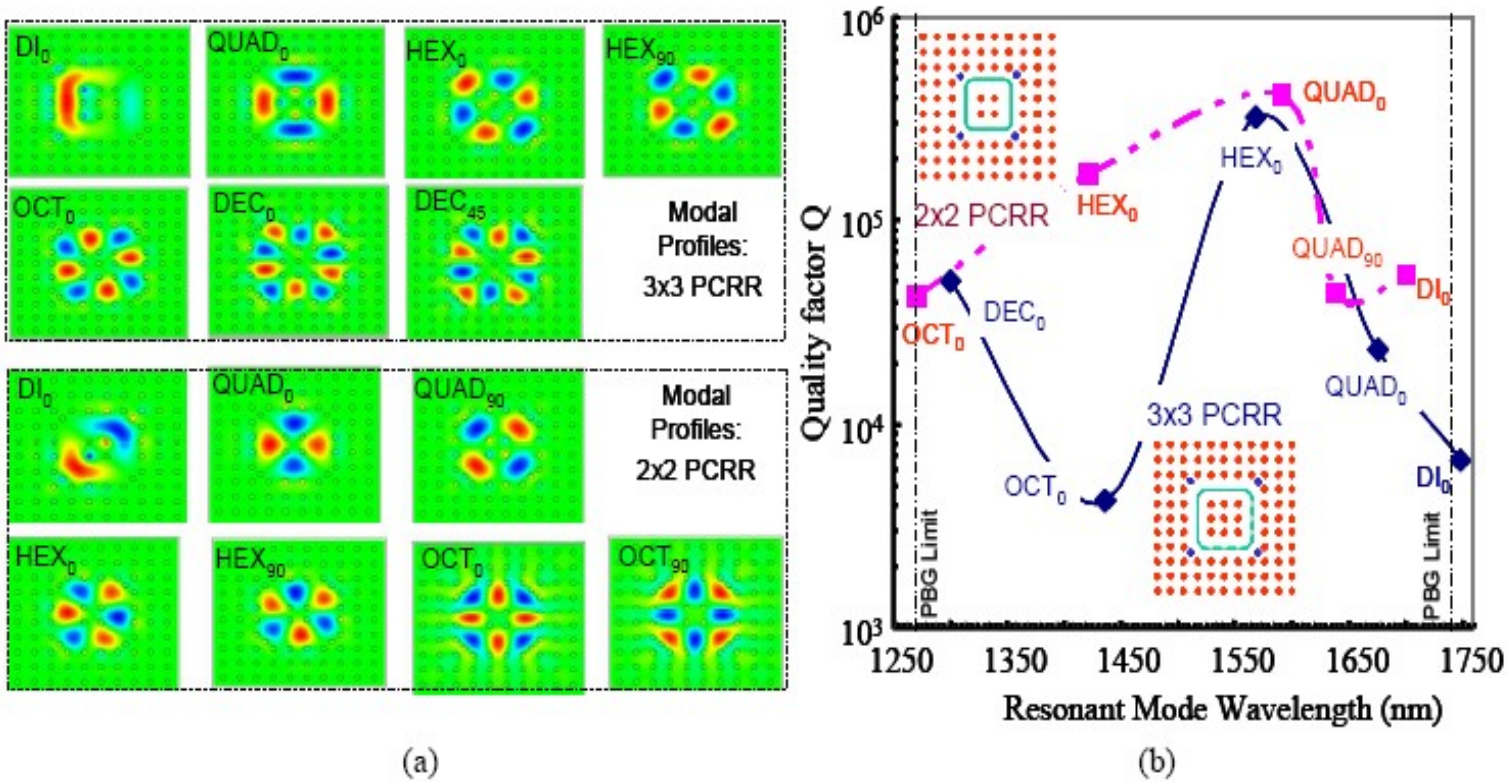

Fig. 2. Modal properties for the quasi-square PCRRs in a square lattice of dielectric rods: (a) Field pattens of the cavity modes within the spectral range of first photonic bandgap; (b) The corresponding resonant mode wavelengths and the quality factor Qs for these modes in both 3x3 and 2x2 PCRRs. The different modes are: dipole (DI), quadrupole (QUAD); hexapole (HEX), octupole (OCT), and decapole (DEC). The modal degeneracy is denoted with the subscript "0" and "90" (or "45").

Single ring: backward drop

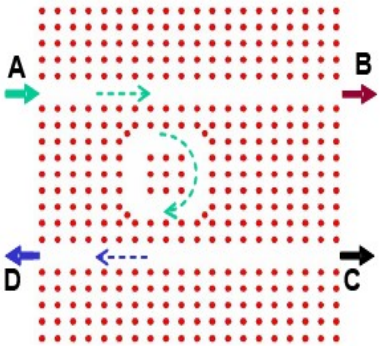

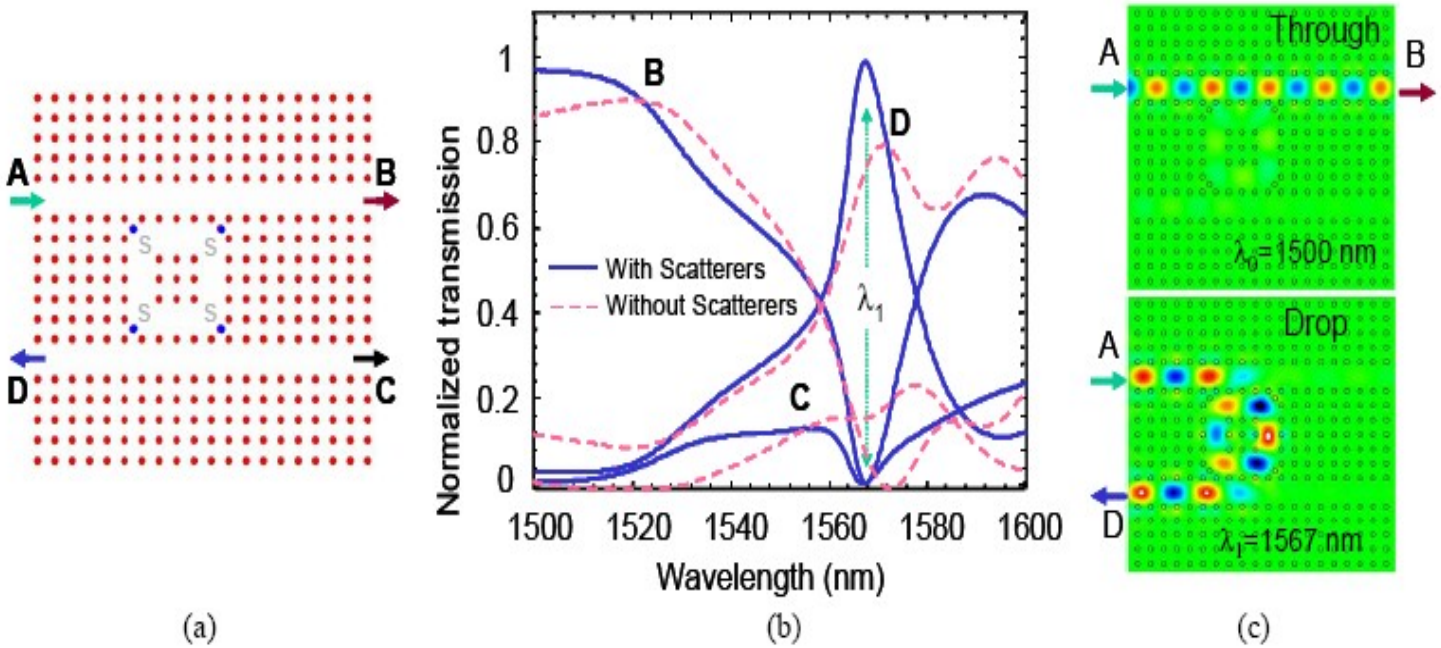

Fig. 4. (a) Single-ring PCRR ADF; (b) normalized transmission spectra at three output ports B, C, D for PCRRs with and without scatterers; (c) The electric field patterns for the through (off-resonance: λ_0=1500 nm) and drop (on-resonance: λ_1=1567 nm) channels.

Micro add/drop filter in photonic crystals

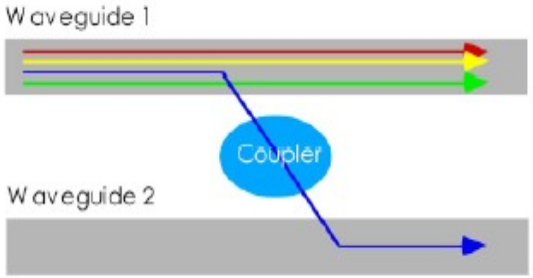

- *Two resonant modes with even and odd symmetry.*
- *The modes must be degenerate.*
- *The modes must have the same decay rate.*

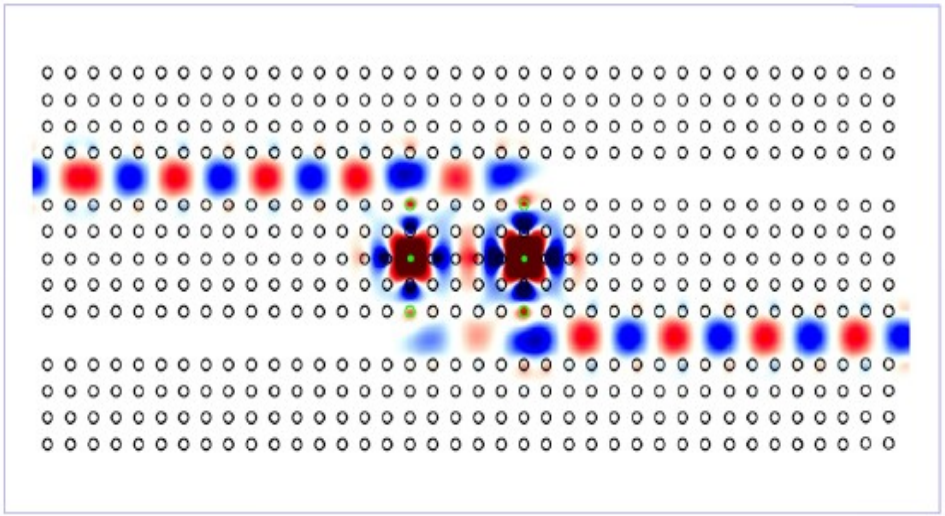

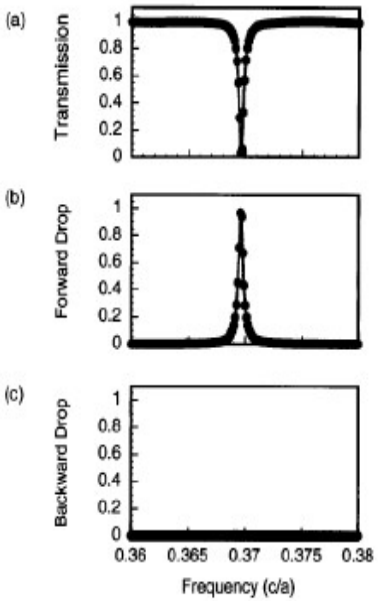

S. Fan, P. R. Villeneuve, J. D. Joannopoulos, and H. A. Haus, Physical Review Letters 80, 960 (1998).

Double ring: forward drop

Double ring: forward drop

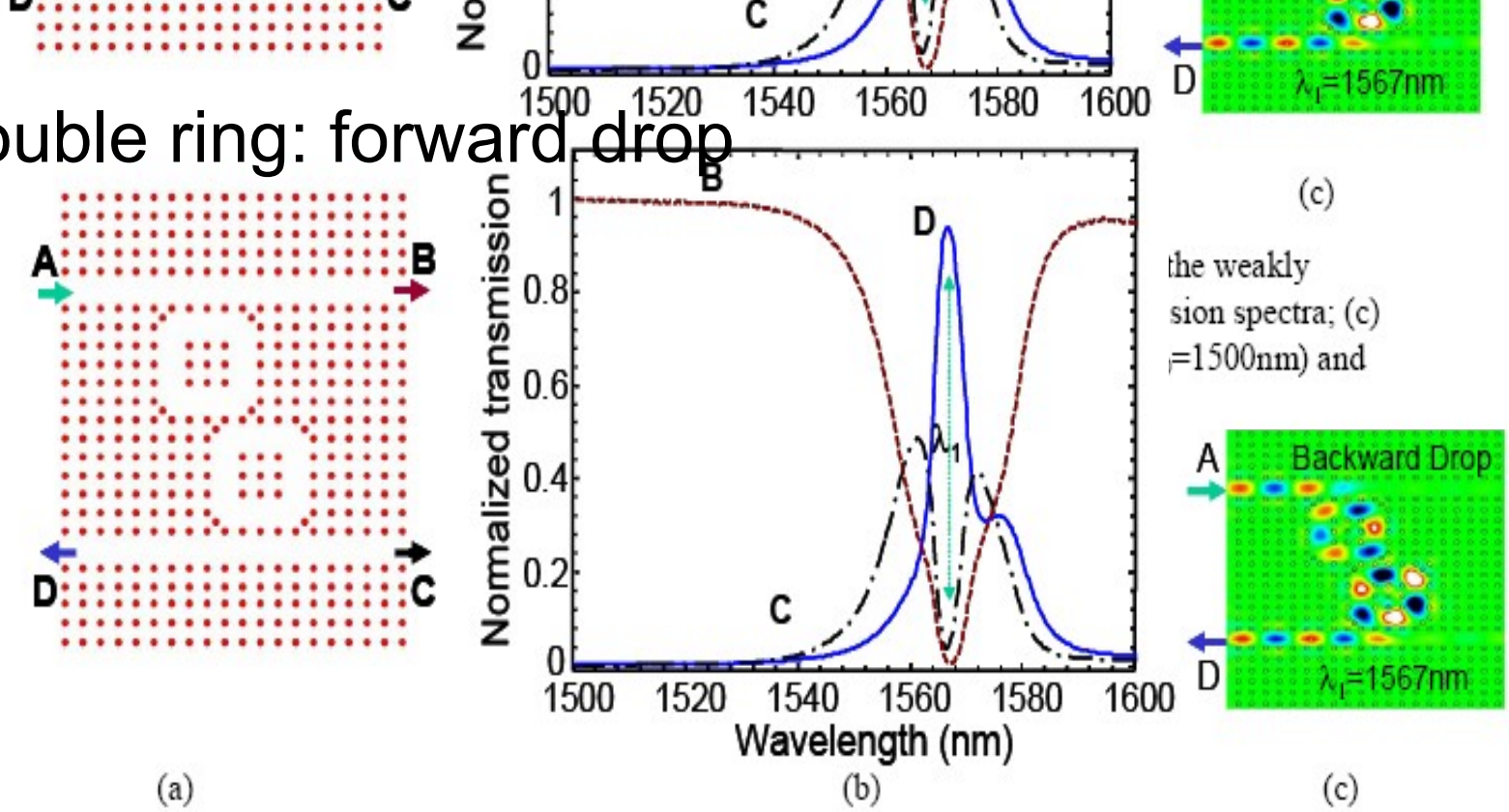

Fig. 6. Dual-ring PCRR ADF for backward-dropping: (a) Schematic showing the weakly coupled dual PCRR rings with coupling period of 2a; (b) Normalized transmission spectra; (c) The field patterns of electric field distribution for "through" (off-resonance: λ_0=1500nm) and "backward drop" (on-resonance: λ_1=1567nm)channels.

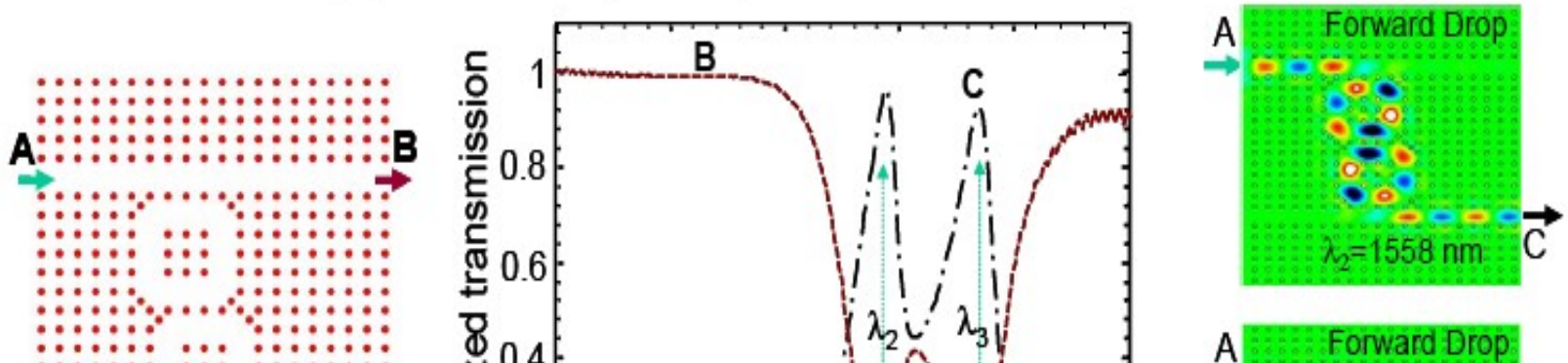

Interconnessione a lunghe distanze

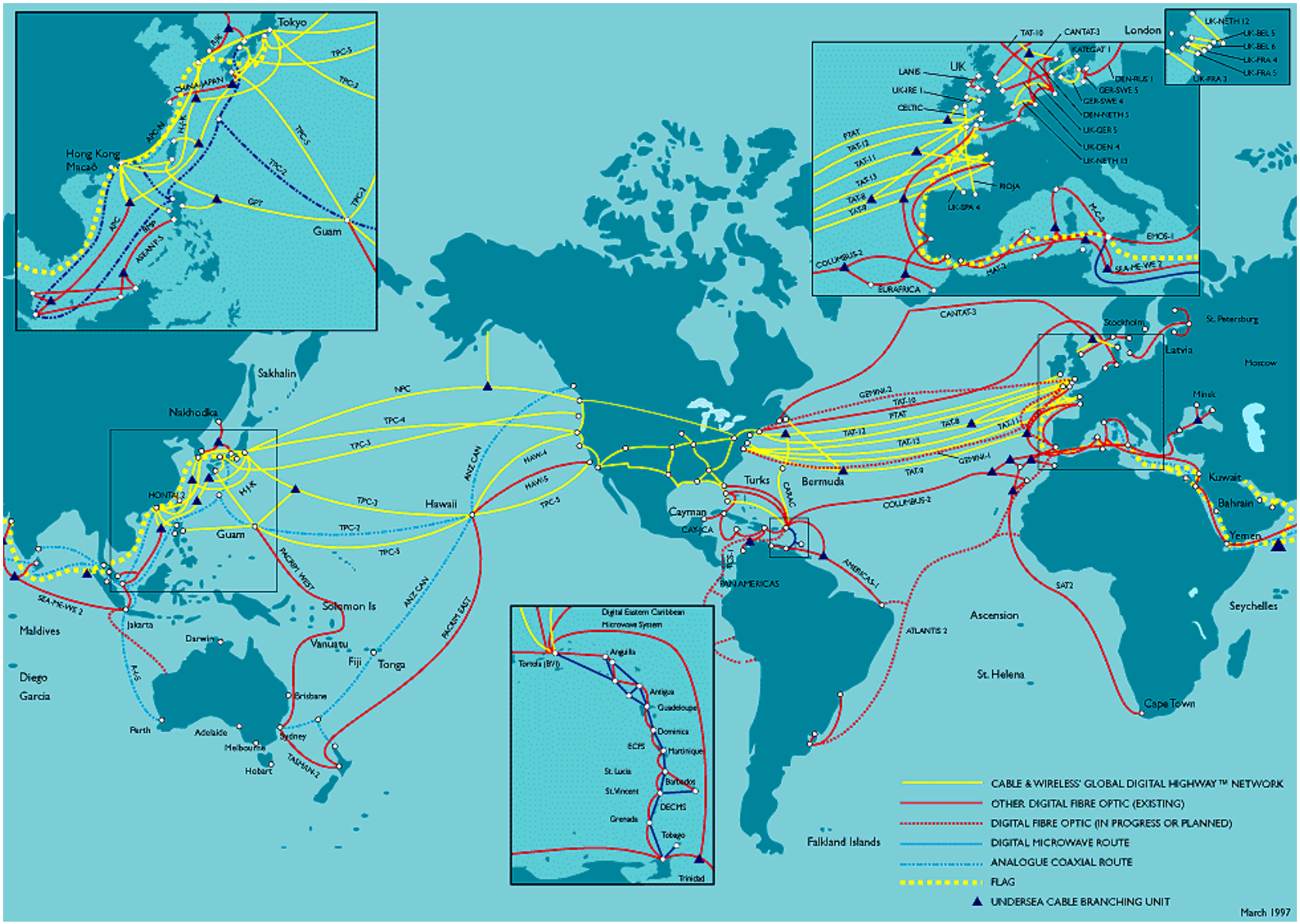

Interconnessione a lunghe distanze

Fibre ottiche

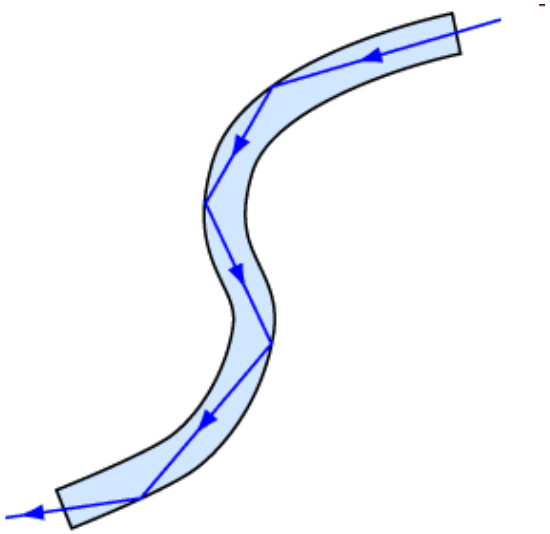

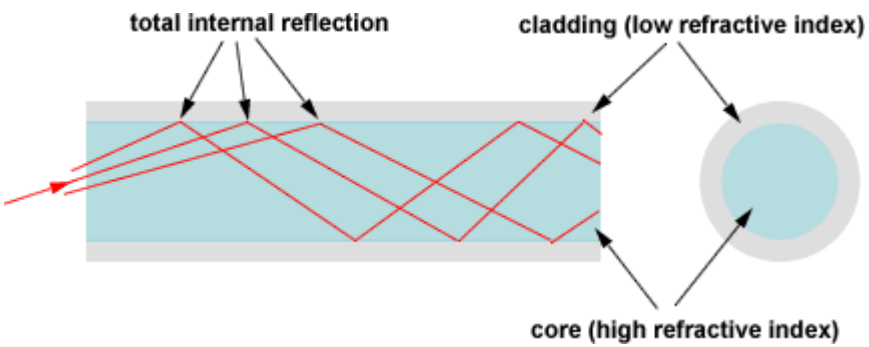

Dielettrico *omogeneo*

Fibre fotoniche

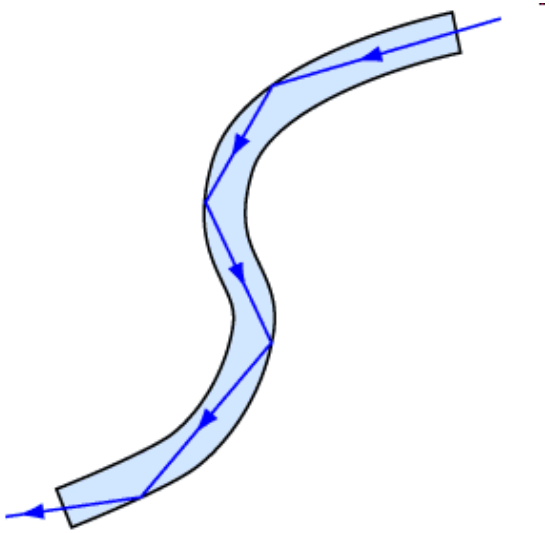

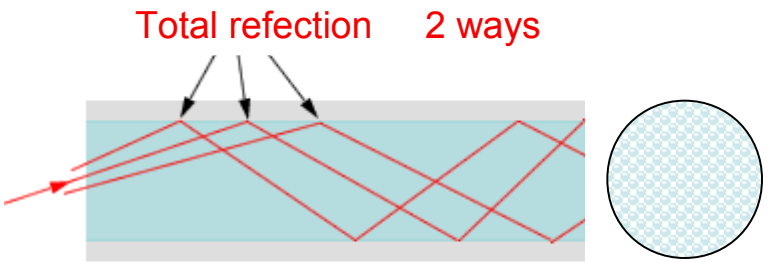

Dielettrico nanostrutturato

Fibre fotoniche

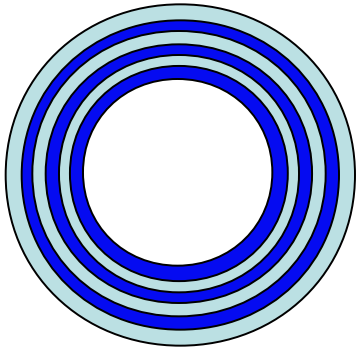

Bragg fibers

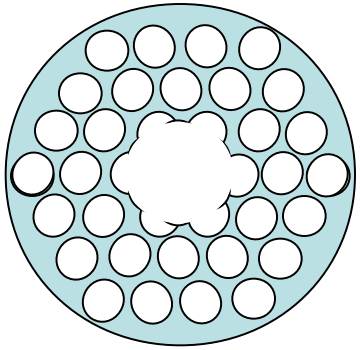

Holey fibers
Hollow core

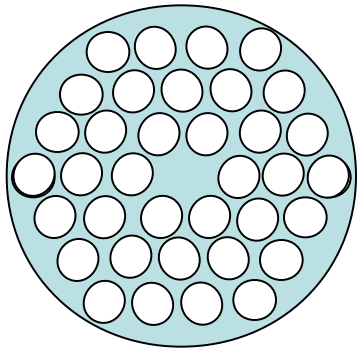

Holey fibers
Solid core

Metodo di fabbricazione

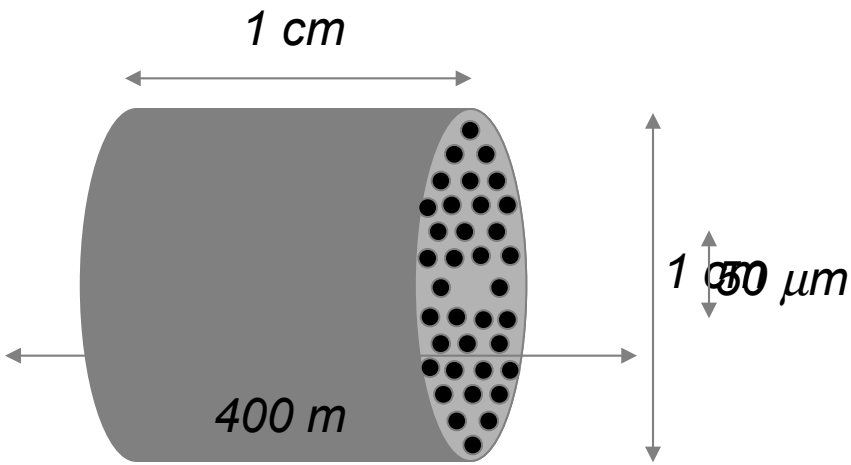

Heating and pulling

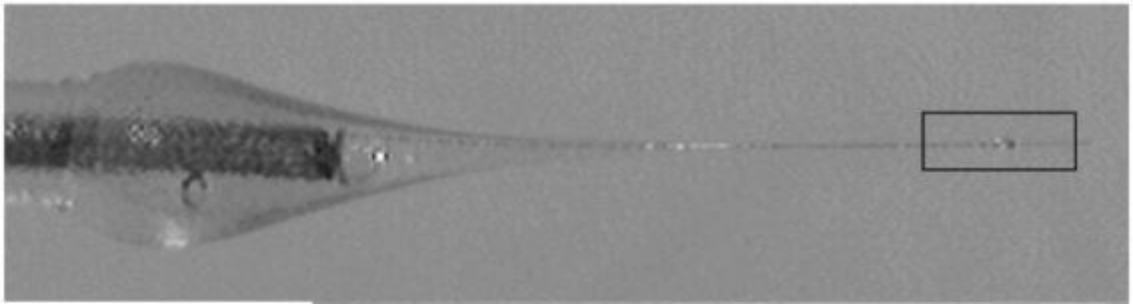

Index Guiding

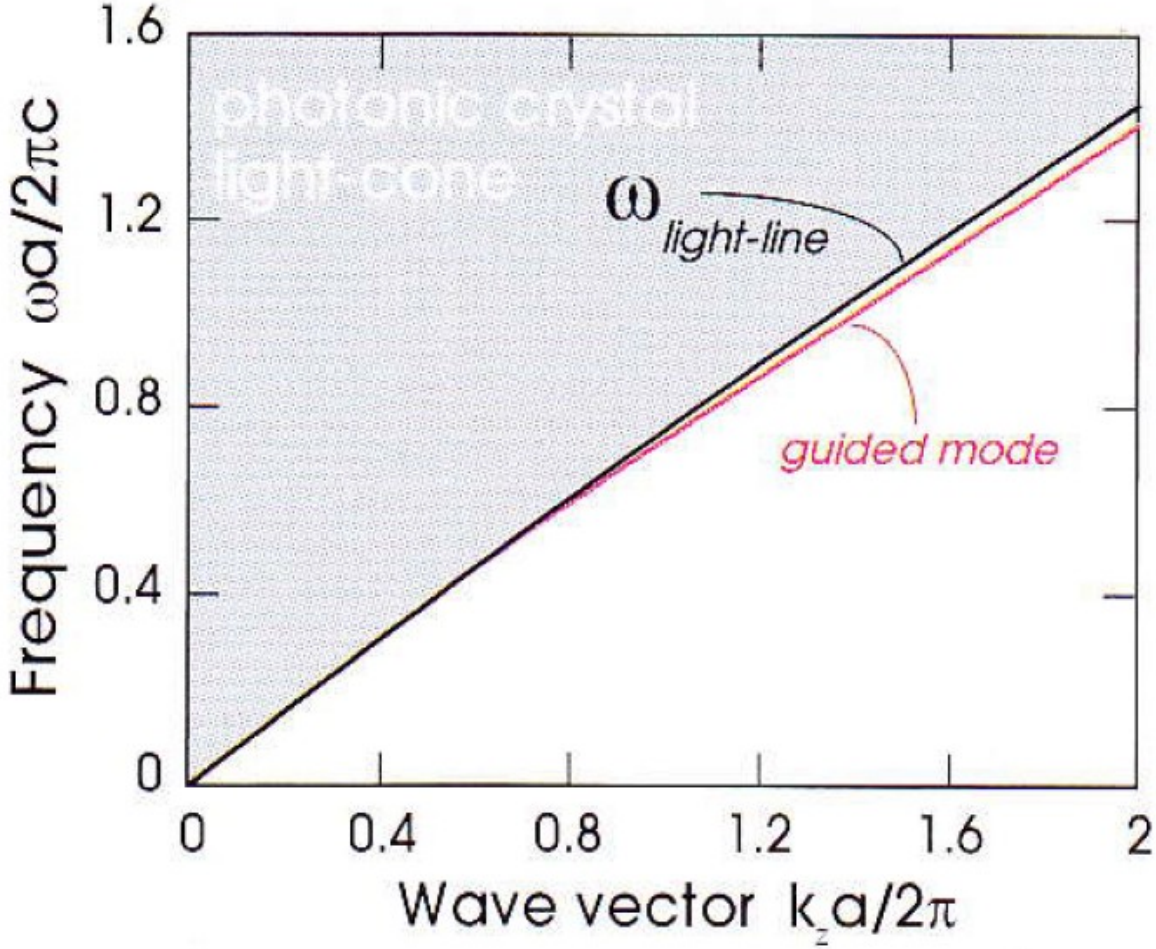

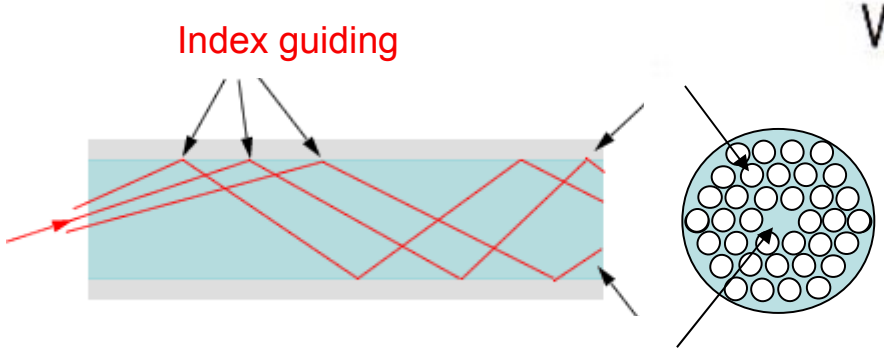

Index Guiding

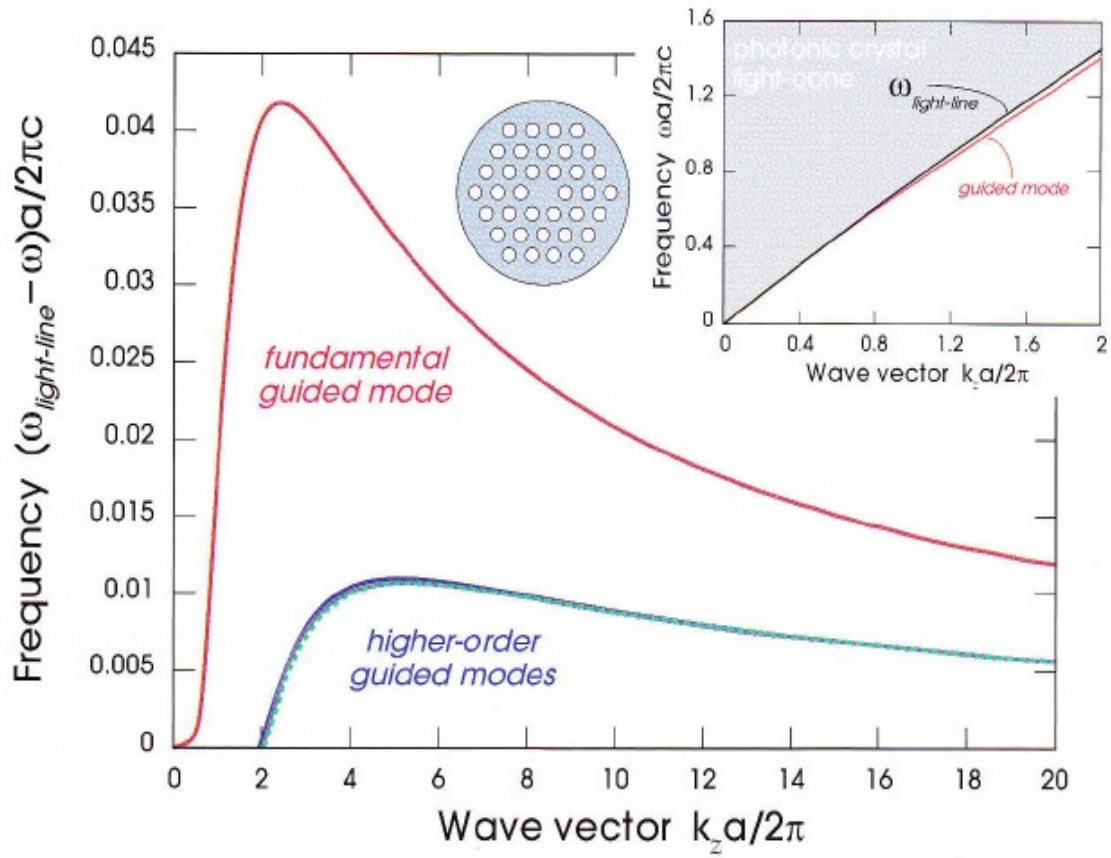

Figure 2: Band diagram of solid-core holey fiber as a function of axial wave vector k_z. The usual ω plot is inset, but for clarity we also plot the $\Delta\omega$ between the guided bands and the light line. The higher-order guided modes are three bands that are nearly on top of one another.

Index Guiding

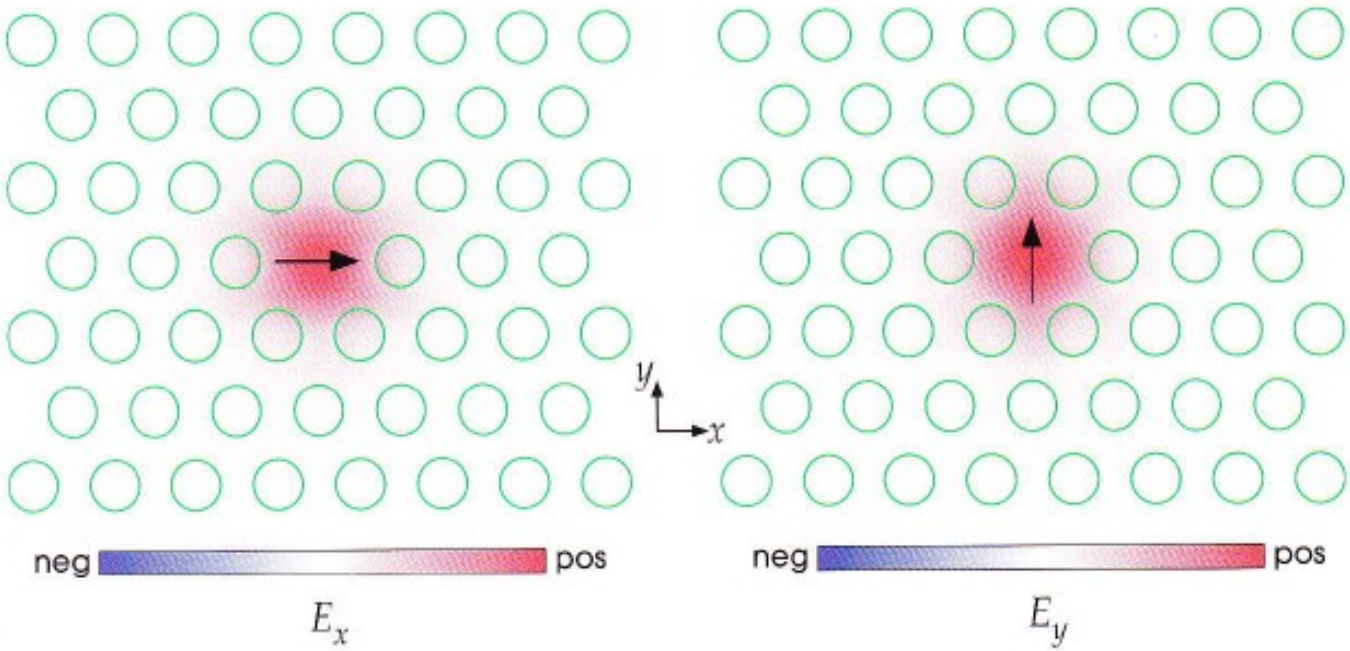

Figure 3: Electric-field pattern for the doubly degenerate fundamental mode of figure 2. Their polarizations are nearly orthogonal everywhere: the mode pictured at left is mostly E_x, and the mode pictured at right is mostly E_y. The green circles show the locations of the air holes.

Endlessly single mode fiber

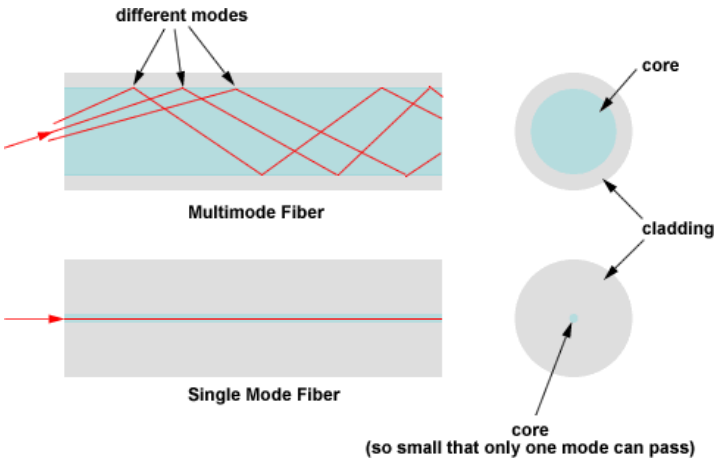

$$\tilde{n}_{eff} = \frac{ck_z}{\omega}$$

Il modo vede n sempre più alto e si confina maggiormente

- Single mode
- Higher NL
- Polarization maintaining

PBG guiding

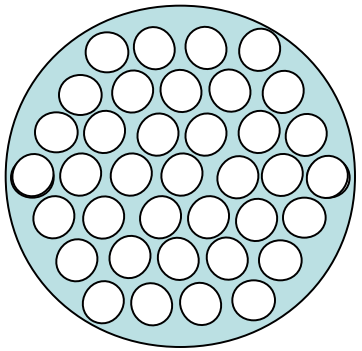

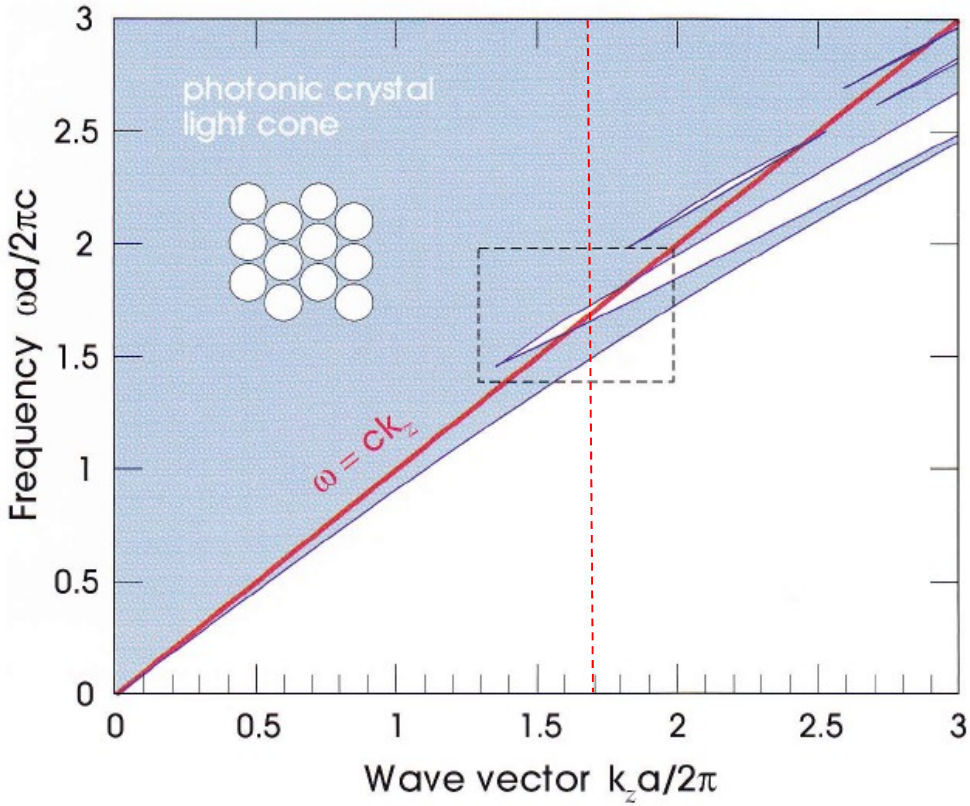

Esiste PBG per propagazione lungo z

Figure 7: Projected band diagram, as a function of out-of-plane wave vector k_z, for a triangular lattice of air holes (inset: period a, radius $0.47a$) in $\varepsilon = 2.1$. This forms the light cone of the holey fiber from figure 1(b), with gaps appearing as open regions. The light line of air, $\omega = ck_z$, is shown in red. (Dashed box indicates region plotted in figures 10 and 12 for the defect modes.)

PI

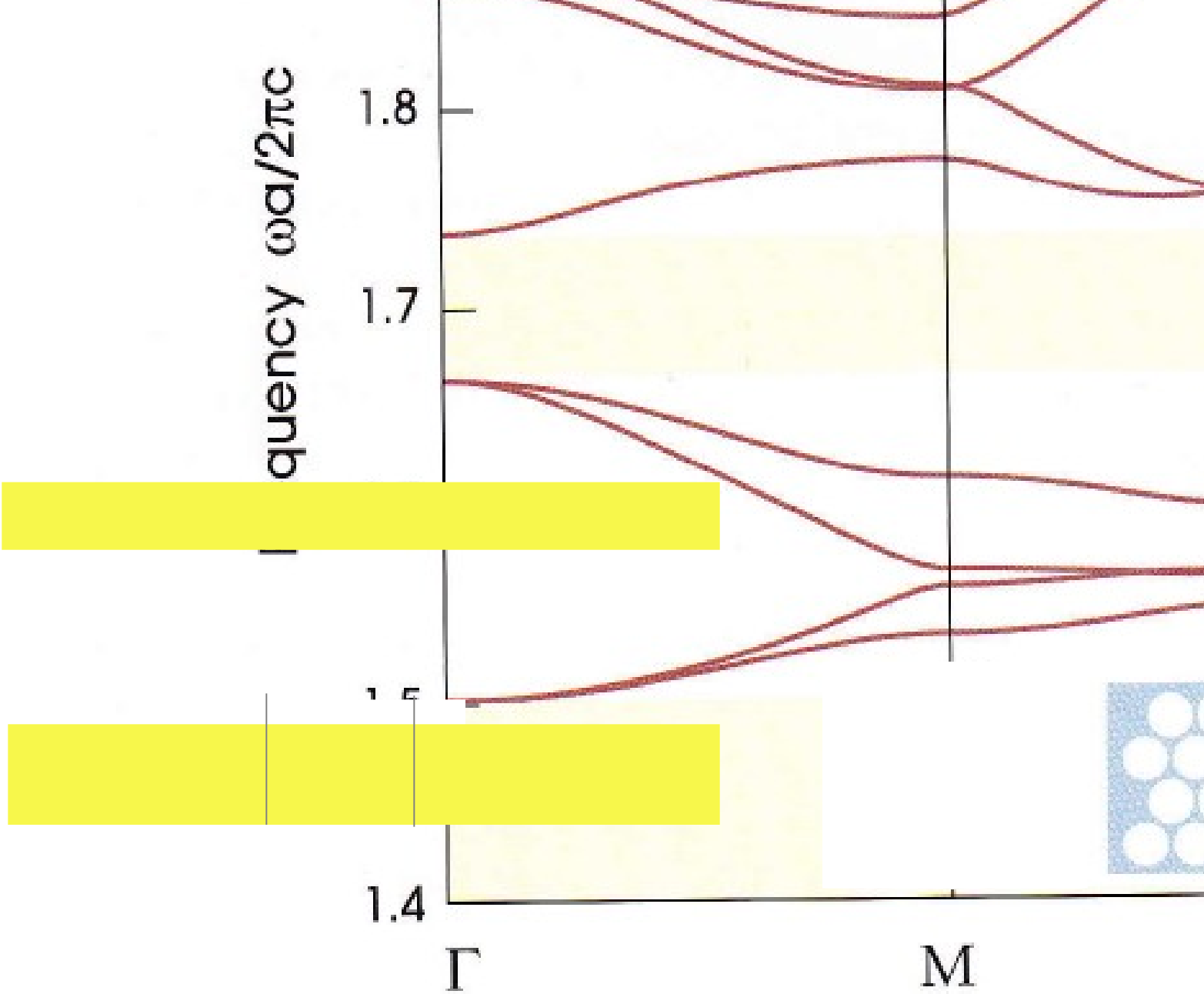

Figure 8
for the tr
$k_z a/2\pi$ =
region, c
where g

Figure 8: Band diagram versus in-plane wave vector i

PBG guiding

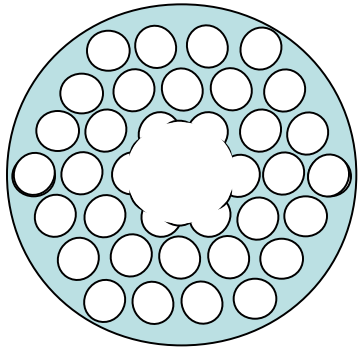

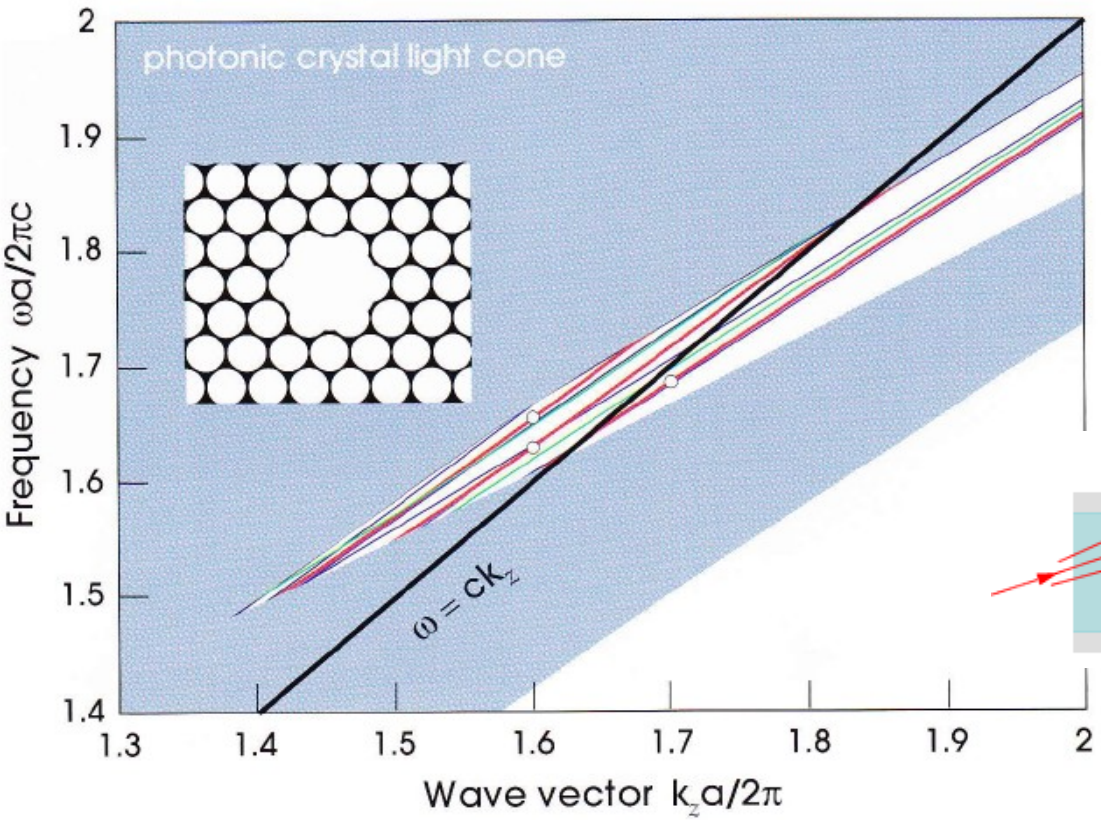

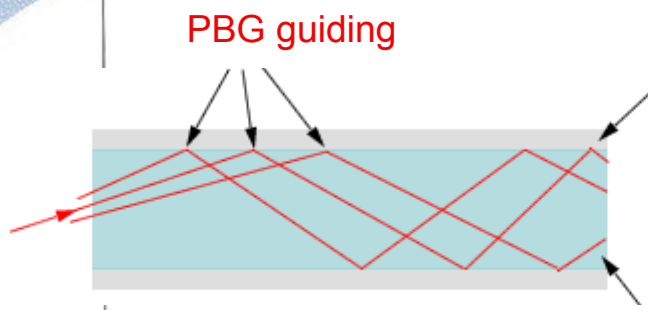

Si introduce un difetto e si ottiene PBG guiding

Figure 10: Band diagram showing guided modes of hollow-core holey-fiber structure (inset, similar to experimental structure of figure 9), corresponding to dashed region of figure 7. (Air core is formed by a radius-1.202a air hole.) Three thick red lines indicate doubly degenerate bands that have the correct symmetry to couple to planewave input light. Thin green lines indicate doubly degenerate bands with a different symmetry, and thin blue lines indicate nondegenerate bands. Bands below the light line (thick black) are surface states confined to the edge of the core. Three dots indicate the modes plotted in figure 11.

PBG guiding

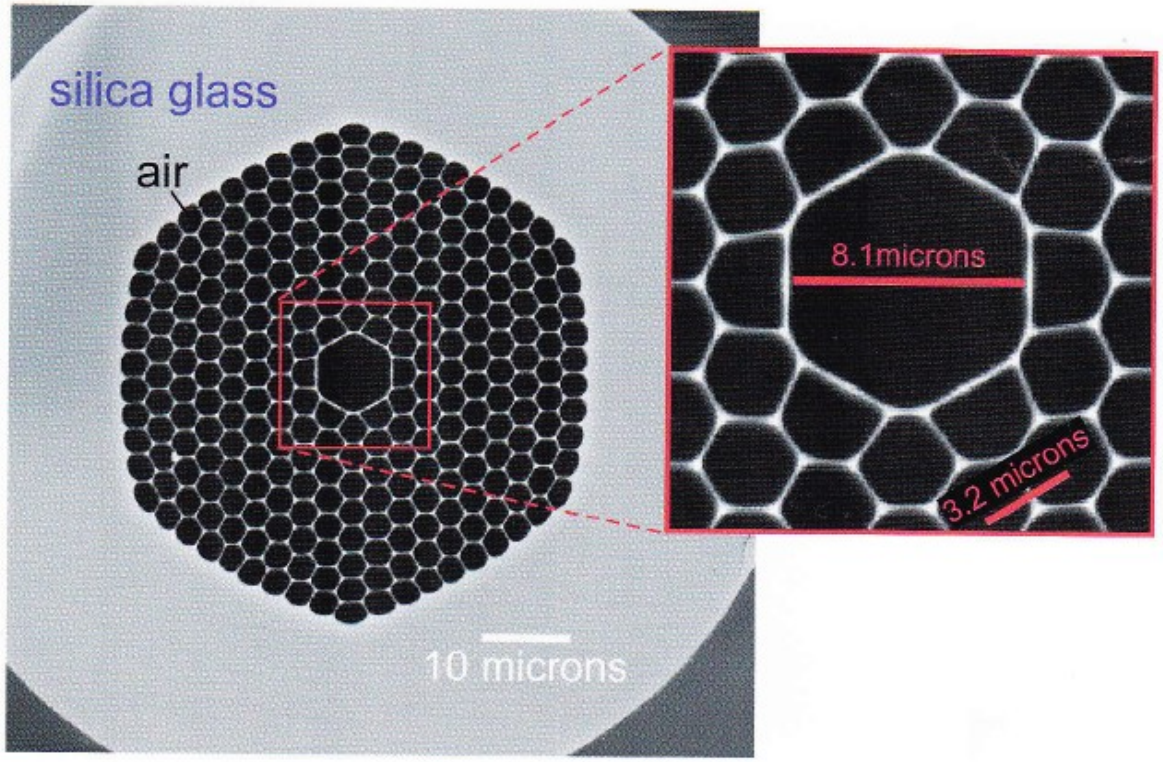

Figure 9: Electron-microscope image of hollow-core holey-fiber cross section (black regions are air holes, and gray regions are silica glass). Central air defect, replacing 7 holes, supports gap-guided modes around a wavelength of 1060 nm. (Image courtesy Karl Koch and Corning, Inc.)

PBG guiding

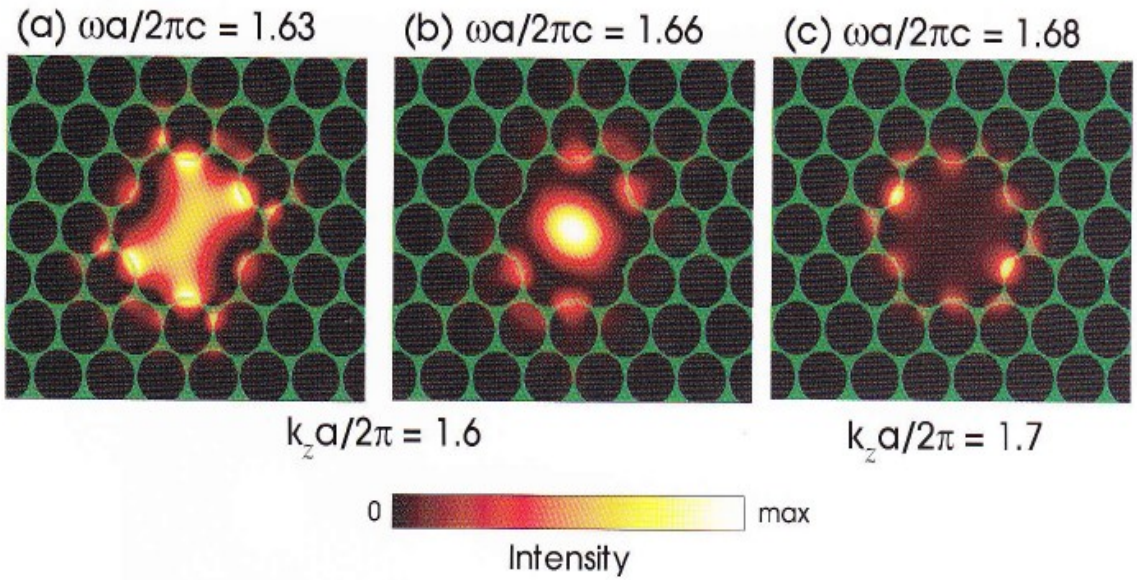

Figure 11: Intensity patterns ($\hat{\mathbf{z}} \cdot \mathrm{Re}[\mathbf{E}^* \times \mathbf{H}]$) of three doubly degenerate modes of a hollow-core holey fiber (ε shaded green), corresponding to the dots on the thick red lines in figure 10. (a) and (b) lie above the air light line at $k_z a/2\pi = 1.6$, while (c) is a surface state lying below the air light line at $k_z a/2\pi = 1.7$.

- Zero absorption for any desired λ
- Insertion of gas, liquid →(sensor)

PBG guiding